processes

MDPI

Review

Supercritical Antisolvent Process for Pharmaceutical Applications: A Review

Paola Franco and Iolanda De Marco *

Department of Industrial Engineering, University of Salerno, Via Giovanni Paolo II, 132, 84084 Fisciano (SA), Italy; pfranco@unisa.it

* Correspondence: idemarco@unisa.it

Received: 8 July 2020; Accepted: 1 August 2020; Published: 4 August 2020

Abstract: The supercritical antisolvent (SAS) technique has been widely employed in the biomedical field, including drug delivery, to obtain drug particles or polymer-based systems of nanometric or micrometric size. The primary purpose of producing SAS particles is to improve the treatment of different pathologies and to better the patient's compliance. In this context, many active compounds have been micronized to enhance their dissolution rate and bioavailability. Aiming for more effective treatments with reduced side effects caused by drug overdose, the SAS polymer/active principle coprecipitation has mainly been proposed to offer an adequate drug release for specific therapy. The demand for new formulations with reduced side effects on the patient's health is still growing; in this context, the SAS technique is a promising tool to solve existing issues in the biomedical field. This updated review on the use of the SAS process for clinical applications provides useful information about the achievements, the most effective polymeric carriers, and parameters, as well as future perspectives.

Keywords: supercritical antisolvent; micronization; coprecipitation; biomedical field; drug delivery

1. Introduction

Nowadays, the focus on novel polymer/drug formulations is continuously growing, in order to improve the therapeutic efficacy of an active compound and to augment the patient's compliance. In this context, the micronization processes provide a robust solution to issues related to the biomedical field, including drug delivery. The use of polymeric carriers to produce composite particles has multiple functions, such as the drug protection against its oxidation and/or deactivation caused by external agents (light, oxygen, temperature, pH) and the masking of unpleasant taste and/or odor. However, the primary motivation is often the modification of the release kinetics of the active principle embedded in the polymeric particles. In the biomedical field, a rapid or a prolonged release of the active compound can be necessary depending on the pathology, which may require a fast or long-term response. Many prescribed active principles have a low solubility in water, resulting in low bioavailability. The particle size reduction, which is achieved by micronizing the active compound, allows improving the dissolution rate of poorly water-soluble drugs [1–7]. However, drug dissolution can be further enhanced by developing polymer-based formulations. This approach is also useful when the active compound cannot be micronized alone [8–13], or when a highly water-soluble drug has to be released slowly. For example, in the case of infections, long-term antibiotic therapies are often prescribed. Unfortunately, many antibiotics are very soluble in water, and are characterized by a very short half-life; in these cases, prolonged-release drug delivery systems are desirable to reduce the number of administration and the unwanted effects, including the antibiotic resistance [14–17]. Instead, given the existence of many inflammatory conditions, in the case of non-steroidal anti-inflammatory drugs (NSAIDs), both a fast and a prolonged release can be required for the treatment of minor

inflammations (e.g., headaches, toothache) or chronic disease (e.g., rheumatoid arthritis, osteoarthritis), respectively [18–20]. However, when NSAIDs are frequently taken, serious side effects may occur, such as nausea, vomiting, gastrointestinal bleeding, and peptic ulcer. All these issues can be solved by controlling the drug release with suitable polymers, which may have mostly hydrophobic or hydrophilic behavior, so producing alternative administration systems.

The typical release kinetics of an active principle from conventional pharmaceutical forms is sketched in Figure 1a, showing how the drug concentration can go below or above the therapeutic range, in an uncontrolled manner. Thus, in this case, high and repeated drug dosages are necessary, leading to serious side effects on the patient's health. In Figure 1b, different release kinetics from alternative drug delivery systems are represented, such as immediate, prolonged, delayed, or pulsed drug releases. In this way, the therapy is targeted for the specific application, and the drug concentration in the plasma is ensured within the therapeutic region, i.e., above the minimum effective concentration (MEC) required to have a therapeutic effect and below the maximum safe concentration (MSC) to avoid toxicities.

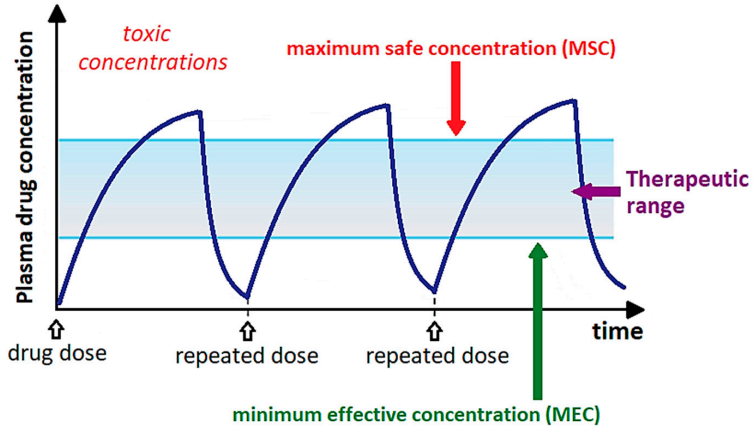

(**a**)

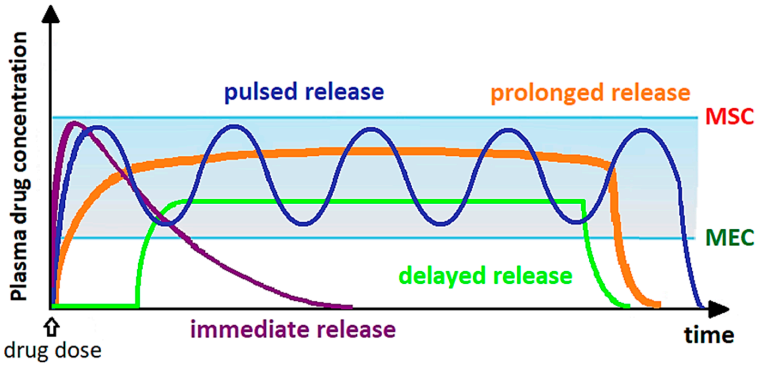

(**b**)

Figure 1. (**a**) Conventional pharmaceutical formulations; (**b**) modified-release drug delivery systems.

There are different technologies to micronize active compounds or to produce composite polymer/drug particles, such as spray drying, freeze-drying, jet-milling, solvent evaporation, or coacervation. Despite the advantages of using these conventional techniques, such as the possibility of scaling up the process without particular complications, in the case of the widely employed spray drying, these methods also present significant limitations [7,12,21–25]. Indeed, multistage processing is often involved to remove the toxic organic solvents used, whose residues are often not negligible in the final product. Moreover, the employed high process temperatures can cause the thermal degradation of the thermosensitive active principles. In addition, using conventional micronization techniques, it is difficult to control the morphology and the dimensions of the produced particles.

On the contrary, these drawbacks can be overcome using processes based on the use of supercritical fluids [7,12,21–25], among which the supercritical carbon dioxide ($scCO_2$) is the most commonly employed in the industrial field. Considerably reducing the use of organic solvents, the $scCO_2$-based micronization techniques permit to produce regular particles of minimal dimensions, which are difficult to obtain with conventional processes.

This goal is possible because, in supercritical conditions, fluids have some gas-like properties (e.g., high diffusivity, low viscosity) and other liquid-like properties (e.g., high density, high solvent power). In particular, the supercritical antisolvent (SAS) technique stands out for the production of nanoparticles and microparticles of one or more compounds in a controlled manner. The first papers on the SAS process date back to the early 90s. For example, Yeo et al. processed para-linked aromatic polyamides obtaining polycrystalline spherulites and microfibrils [26,27], Bertucco et al. obtained hyaluronic acid benzylic ester microspheres that can be used for controlled drug delivery [28], Reverchon et al. obtained nanoparticles and sub-microparticles of different superconductor precursors [29,30].

Regarding the pharmaceutical field, using the SAS process, up to now, micronized drug particles and several polymer/active compound composites have been proposed for different biomedical applications [31–35]. Indeed, SAS precipitated particles can be used for drug delivery by oral, parenteral, transdermal, or topical routes [2,36–42]. The versatile SAS particles can be used in powder form for the oral administration of composites or the preparation of aerosol formulations, mainly for the treatment of respiratory diseases; they can also be used for the production of medicated patches or active topical gels, by incorporating nanoparticles/microparticles into various types of dressings, supports or pomades, respectively. The dissolution kinetics of many active principles, both of synthetic and natural origin, have been successfully modified by selecting carriers suitable for the required therapy. Different biopolymers, which are biocompatible [11,22,43,44] and sometimes even biodegradable [32,45–49], have been studied to tune the release of the active compounds. In literature, there are few reviews about the SAS technique [50–53]. An older overview [53] was focused on the precipitation of single compounds in the form of microparticles and nanoparticles, mainly introducing the fundamentals of the SAS technique. In this study, the micronization of different kinds of materials was considered, without choosing a specific field of application. Abuzar et al. [50] focused their attention to poorly water-soluble drugs, recommending the SAS process as an innovative tool to enhance the bioavailability of these active principles. In another review [51], the SAS process has been indicated as a promising drug encapsulation method, but a limited number of studies compared to the existing ones have been analyzed. Moreover, the crucial role of the polymeric carrier to produce novel formulations for specific biomedical applications and drug dissolution rate is not highlighted. In the paper of Gonzalez-Coloma et al. [52], the attention was instead given to the supercritical antisolvent fractionation (SAF) of natural products. The SAF process is conceptually similar to the SAS one since, in any case, the supercritical fluid acts as an antisolvent; however, the difference is that, in the former technology, a complex mixture consisting of various compounds in a solvent has to be selectively fractionated, precipitating a compound or a series of compounds of interest. It has to be considered that none of the aforementioned reviews report the interesting results obtained in recent years, such as the new carriers identified, whose use has been optimized lately.

Considering the advantages associated with the use of the SAS technique and the goals achieved so far, it is clear that this technology can still make a significant contribution to improving the treatment of several diseases. Therefore, this updated review is focused on the application of the SAS process in the medical/pharmaceutical field, both regarding the micronization of active compounds and their coprecipitation with polymeric carriers. The advantages and disadvantages associated with the use of the SAS technique, the most effective polymeric carriers, and operating conditions, as well as the processed active principles and the potential applications, are indicated. This review provides guidelines for future prospects.

2. SAS Process: Fundamentals and Test Procedure

The SAS process is based on some main prerequisites. In this technique, the $scCO_2$ has the role of the antisolvent; therefore, it has to be completely miscible with the selected liquid solvent. On the contrary, the solute/solutes to be processed has/have to be soluble in the liquid solvent but insoluble in the binary mixture formed in the precipitator consisting of the solvent and the antisolvent. Hence, the precipitation/coprecipitation of solute/solutes occurs because of the fast diffusion of $scCO_2$ into the liquid solvent and the consequent supersaturation of the solute/solutes.

A schematic representation of the SAS process is reported in Figure 2. Briefly, a typical SAS experiment begins by pumping the CO_2 to reach the desired pressure in the precipitator, which is heated up to the selected temperature. Once the operating conditions are stabilized, the pure solvent is delivered to the precipitator, passing through a nozzle. Then, the liquid solution, which consists of the solute/solutes dissolved in the selected solvent, is injected. Due to the supersaturation, the solute/solutes precipitate on a filter, whereas the mixture solvent/antisolvent is recovered and separated downstream the precipitator, where a vessel to collect the liquid solvent is located. Once the solution is injected, the $scCO_2$ continues to flow to eliminate the solvent residues. At the end of this washing step, the precipitator is depressurized down to atmospheric pressure, and the precipitated powder can be collected.

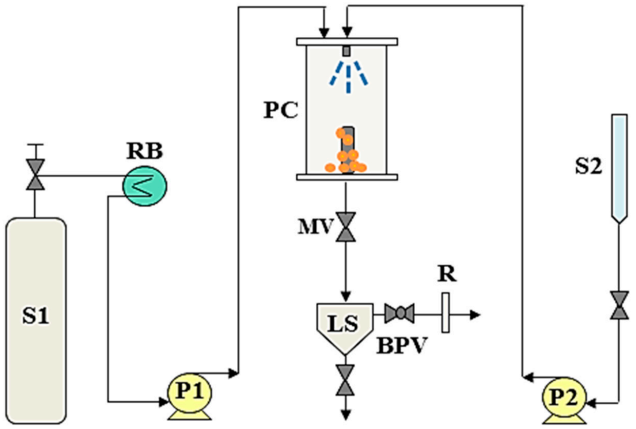

Figure 2. A scheme of the supercritical antisolvent (SAS) apparatus. P1, P2: Pumps; S1: CO_2 supply; S2: Liquid solution supply; RB: Refrigerating bath; PC: Precipitation chamber; LS: Liquid separator; MV: Micrometric valve; BPV: Back-pressure valve; R: Rotameter.

There are also some modified versions of the SAS technique, in which the $scCO_2$ acts equally as an antisolvent, such as the supercritical gas antisolvent (GAS) process and the solution enhanced dispersion by supercritical fluids (SEDS). In the SEDS process, the $scCO_2$ and the liquid solution are both injected through a coaxial nozzle. Instead, in the GAS process, the $scCO_2$ is introduced into the solution consisting of solute/solutes to be precipitated and the liquid solvent. The SAS process was also proposed in the literature with other different acronyms, such as the aerosol solvent extraction system (ASES).

3. SAS Micronization of Active Compounds

Different factors can influence the oral bioavailability of an active compound, including the first-pass metabolism, the drug permeability, and its solubility and dissolution rate in water [54]. In particular, poor solubility and slow dissolution rates are the leading causes of the low bioavailability for most of the active principles [55–57]. Consequently, a low drug amount, often at an insufficient concentration, is available at the specific site of action.

In the last decades, drug particles with nanometric or micrometric size have been applied to treat or prevent different pathologies or medical conditions. As previously mentioned, the micronization of an active compound revealed to be a possible approach to enhance its dissolution rate, since the particle size reduction leads to an increase of the specific surface area in contact with the aqueous solution.

Most of nonsteroidal anti-inflammatory drugs (NSAIDs) are a striking example of poorly-water soluble drugs. The micronization of active principles is also a valid solution to reach a target part of the body. Aerosol drug administration or anticancer therapies are striking applications. The drug micronization is also a valid solution when a specific range of particles' size is required for a certain disease; for example, in the case of pulmonary diseases, drug particles (e.g., antibiotics) with mean diameters lower than 1 μm and a controlled particle size distribution (PSD) are desirable.

For these purposes, the SAS technique is one of the most effective micronization techniques based on the use of supercritical CO_2. Up to now, several active compounds, such as antibiotics [25,58–64], NSAIDs [46,65], antioxidant compounds [1,6,7,38,66], anticancer drugs [3,4,67–69], and others [2,32,70–72], were micronized in the form of nanoparticles, sub-microparticles, and microparticles using the SAS process.

As in the case of the other supercritical fluids assisted technologies, SAS micronization allows overcoming the main drawbacks of conventional micronization techniques, such as spray drying, freeze-drying, jet-milling, solvent evaporation, and grinding [7,25]. For example, Rogers et al. [73] focused their review on a comparison between $scCO_2$-based processes, including SAS, and cryogenic spray-freezing technologies in the micronization of active principles. Both approaches were presented as potential solutions for the production of particles of active compounds that cannot be processed by conventional micronization techniques, such as spray drying and jet-milling. However, the authors highlighted the advantage of using an environmentally-friendly antisolvent as the $scCO_2$ (in the specific case of the SAS technique) compared to the organic and toxic antisolvents conventionally employed. Moreover, the gas-like and liquid-like properties of $scCO_2$, such as the high diffusivity and the high solvent power, allow obtaining dry particles without solvent residues in one step. In reverse, lyophilization or liquid antisolvent extraction are needed to dry powders prepared by the cryogenic micronization technologies. The study of Park et al. [25] demonstrated the superiority of the SAS process with respect to spray drying in the micronization of cefdinir (a model drug). Indeed, microparticles with a mean size equal to 2.32 ± 1.76 μm were obtained by spray drying, whereas nanoparticles with a narrow PSD (0.15 ± 0.07 μm) were produced by the SAS process. Moreover, the specific surface area of SAS-processed particles (55.79 ± 0.06 m^2/g) was higher than that of spray-dried particles (35.01 ± 0.63 m^2/g). The increase in the surface area led to a better contact with the water molecules, so the dissolution of the SAS-processed cefdinir was faster than the spray-dried drug particles. According to the results obtained by Ha et al. [7], SAS micronization also proved to be more effective than milling techniques. Indeed, SAS nanoparticles and sub-microparticles (size in the range: 0.15–0.50 μm) allowed to speed up the dissolution of resveratrol, with respect to crystals (18.75 μm) or crystals/irregular coalescent particles (1.94 μm) produced by Fritz milling and jet-milling, respectively. Therefore, it is ascertained that SAS micronization provides benefits in the final pharmaceutical product both in terms of morphology and dimensions of the particles that constitute it.

Similarly, in other works [1–7,38,66,72,74–77], the SAS micronization led to an enhancement of the drug dissolution rate; in some cases, a slight improvement was already observed even when smaller crystals and no regular particles were obtained by SAS with respect to the unprocessed drug. The SAS technique offers the possibility of obtaining both crystalline and amorphous materials by modulating the operating conditions of pressure and temperature. For example, at a fixed temperature, crystals mostly precipitate working at pressures below the mixture critical point (MCP) of the drug/solvent/$scCO_2$ system, i.e., in the biphasic region. The possibility of producing an amorphous material increases by increasing the pressure, up to a value much higher than the critical pressure, i.e., at fully-developed supercritical conditions. The attainment of amorphous powders involves numerous benefits, including the enhancement of the drug dissolution rate in an aqueous environment, due to a higher contact between the water molecules and the active principle with an increased specific surface area.

However, as emerged from several papers, the selection of the proper liquid solvent is crucial. Indeed, the success of SAS precipitation strongly depends on the affinity between the solvent and the supercritical antisolvent, i.e., the solubility of the liquid solvent in the supercritical CO_2 and the fast gas-like diffusion of the supercritical CO_2 in the solvent. These fundamental aspects assure

the attainment of small particles. Many studies showed that dimethylsulfoxide (DMSO) is one of the best solvents for SAS micronization [1,3,6,17,46,58–62,65,67,71], as it often allows to produce particles with good morphology and small size, in addition to being the most used solvent. Respecting the basic prerequisites of SAS precipitation, up to now, DMSO allowed micronizing a wide variety of active principles in the form of nanometric and micrometric particles. Ethanol [5,7,63,64,69,78] and acetone [2,68] also emerged as good solvents for the SAS micronization of active compounds. In addition, some active principles were effectively micronized using methanol [7,25,72] and N-methyl-2-pyrrolidone (NMP) [38,58,60]. Moreover, acetone belongs to the category of solvents that have a narrow pressure range to switch from the two-phase to the single-phase mixing with $scCO_2$; using this kind of solvent, nanoparticles are generally obtained [79]. Instead, microparticles usually precipitate with DMSO, EtOH, and NMP, which are solvents that present a broad transition zone from the two-phase to the single-phase mixing with $scCO_2$. For the latter category of solvents, high operating pressures are necessary to produce nanoparticles. In some papers, SAS precipitation was also attempted by solubilizing drugs into solvent mixtures, which consisted of the solvents above, but satisfying results were reached only in few cases [1,7,13,59,66,80,81].

Another critical parameter for a successful micronization is the molar fraction of CO_2, which should allow the complete miscibility between the solvent and the antisolvent at the selected pressure and temperature. For this purpose, in most of the reported papers, CO_2 molar fractions higher than 0.95 were used. In addition, the operating pressure and the concentration of the active compound in the liquid solution also influence the morphology and the size of the precipitated powders. In particular, when spherical particles are produced, a decrease of the pressure or an increase of the drug concentration often results in an increase of particles' dimensions [5,38,58,61,62,69,72]. However, it is possible that large crystals significantly precipitate, increasing drug concentration. This result can be explained considering that the presence of the active compound can modify the high-pressure vapor-liquid equilibria (VLEs) of the solvent/antisolvent binary system.

Consequently, the MCP of the drug/solvent/$scCO_2$ ternary system shifts towards higher pressures with respect to the MCP of the solvent/$scCO_2$ binary system [82,83]. Therefore, the operating point could lie below the MCP, i.e., in the biphasic region. This effect is accentuated by increasing the drug concentration in the liquid solvent.

The morphology and the dimensions of SAS-processed particles obviously will influence the dissolution of the active compound. Indeed, as highlighted in various papers [7,38,66,72], a smaller particle size, which means an increased surface area, led to an increase in the drug dissolution rate.

SAS particles can be used for oral, parenteral, and topical drug administration; in the latter case, the micronized drug particles can be incorporated into various types of dressings or supports. Up to now, SAS-micronized drugs were proposed for different diseases or clinical conditions, including inflammations and pains [11,12,75,84], infections [2,4,25,58,59,61,63,64,74,77,85,86], diabetes [5,7,66], psychological disorders [87], asthma [32,71,88], tumors [1,3,4,31,38,67–69,78,89–92], cardiovascular pathologies [6,33,70,76], etc.

However, some active compounds are not processable by the SAS technique. Indeed, in many cases, SAS micronization substantially fails since crystals precipitate [11–13,74,87,90,93] or, even, the active compound can be extracted by the solvent/$scCO_2$ mixture [8,9] not respecting the fundamental prerequisites of the SAS process.

Nevertheless, different studies proved that it is possible to force the morphology of these compounds not suitable for SAS micronization through their coprecipitation with a proper selected polymeric carrier [5,8–13,44].

In Table 1, a summary of the active compounds processed by SAS micronization is reported. The active principle to be micronized, the morphology and size of precipitated powders, as well as the applications are indicated. The operating conditions that mainly influence the morphology of particles are also specified, i.e., the liquid solvent used, the pressure (P), the temperature (T), and the drug concentration in the injected solution (C).

Table 1. An overview of SAS micronization of active compounds. C: Crystals; NP: Nanoparticles; SMP: Sub-microparticles; MP: Microparticles; BL: Balloons; c: Coalescent; AGG: Aggregates; m.s.: Mean size; NSAID: Nonsteroidal anti-inflammatory drug; DLBS2347: Manilkara kauki L. Dubard's leaf extract; HCPT: 10-Hydroxycamptothecin; GBE: Ginkgo biloba extract; AC: Acetone; CHF: Chloroform; EtAc: Ethyl acetate; EtOH: Ethanol; DMSO: Dimethylsulfoxide; DCM: Dichloromethane; DMFA: N,N-dimethylformamide; MeOH: Methanol; NMP: N-methyl-2-pyrrolidone; iPrOH: Isopropanol; THF: Tetrahydrofuran.

Active Compound	Solvent	P [MPa]	T [°C]	C [mg/mL]	Morphology	Applications	Reference
Risperidone	CHF	5–20	40	25–100	C (size: 10–200 μm)	antipsychotic to treat bipolar and obsessive-compulsive disorders, schizophrenia	[87]
Sulfathiazole	AC, EtOH	10–14	35, 45, 55	3–13	C+MP (m.s.: 2.1–16.9 μm)	antimicrobial drug	[2]
Paracetamol	MeOH	10	40	Not reported	C (size: 4.2 μm)	analgesic and antipyretic to treat fever, headaches, and others	[75]
Cefonicid, Cefuroxime, Cefoperazone	DMSO	9–18	40–60	10–90	SMP, MP or BL of Cefonicid and Cefuroxime SMP or MP of Cefoperazone (size: 0.1–50 μm)	cephalosporins used before-surgery, to treat pneumonia, skin infections, urinary tract and post-operative infections	[61]
Ampicillin	NMP, EtOH, DMSO	8–15	40	20	SMP, MP, cSMP, irregular MP (m.s.: 0.26–1.2 μm)	antibiotic to treat respiratory, gastrointestinal and urinary tract infections	[58]
Amoxicillin	DMSO, DMSO/EtOH, DMSO/MeOH	10–25	40	0.005–0.02	SMPs, MPs (size: 0.2–1.6 μm)	antibiotic to treat infections of the skin, urinary and respiratory tracts	[59]
Amoxicillin	NMP, DMSO	15	40	20–100	SMP, MP (m.s.: 0.25–1.2 μm)		[60]
Ampicillin, Amoxicillin	DMSO	9	40	20	SMP (m.s.: 0.23 μm for Ampicillin, 0.26 μm for Amoxicillin)	antibiotics	[17]
Griseofulvin, Ampicillin, Amoxicillin, Tetracycline	NMP, DMSO, EtOH, DCM	10–18	40	20–120	C of Griseofulvin AGG of Ampicillin Film of Amoxicillin cSMP of Tetracycline (m.s.: 0.2–0.6 μm)	Antibiotics for various infections	[85]
Griseofulvin	THF, DCM	9.7	35	5	C, needles, irregular NP-SMP (m.s. 0.13–0.51μm)	Antibiotic and antifungal drug	[86]
Cefdinir	MeOH	12	45	20	NP (m.s.: 0.15 μm)	antibiotic to treat infections of skin, eyes and respiratory tract	[25]

Table 1. *Cont.*

Active Compound	Solvent	P [MPa]	T [°C]	C [mg/mL]	Morphology	Applications	Reference
Rifampicin	DMSO, NMP, MeOH, EtAc, DCM	9–14.5	40	5–70	C, SMP, MP (m.s.: 0.4–5.0 μm)	antibiotic to treat tuberculosis, meningitis, biliary tract infections	[62]
Minocycline hydrochloride	ethanol	7.5–13	35–50	1–20	cSMP/AGG (m.s.: 0.2–0.3 μm)	antibiotic to treat infections of skin, urinary and respiratory tracts	[63,64]
Moxifloxacin	DMSO, DMFA, MeOH, acetic acid	15	40	1–50	C (m.s.: 0.3–8.2 μm)	antibiotic to treat tuberculosis	[77]
Sulfamethoxazole	AC	10–12	35	88	C (m.s.: 42–5 μm)	antibiotic to treat urinary tract infections, otitis, shigellosis, interstitial pneumonia	[74]
Theophylline	DMSO	9	40	20	C	bronchodilator to treat asthma	[44]
Salbutamol	DMSO, MeOH, EtOH/H_2O	9.5–15	40	3–10	BL, cMP, rods (length: 1–3 μm; diameter: 0.2–0.4 μm)	drug to treat bronchial asthma	[71]
Fluticasone propionate	DCM	6.5–11	40–60	5–17	C (m.s.: 3.7–9.1 μm)	corticosteroid to prevent asthma symptoms	[88]
Dexamethasone, prednisolone, budesonide	EtOH	9–15	40	20	C	corticosteroids to treat ocular and pulmonary diseases, hepatitis, ulcers	[93]
Budesonide	DMC	7.9–13.9	35–45	0.002–0.01	AGG, MP (m.s. 1.4–2.0 μm)	corticosteroid to treat asthma, nasal polyps, bronchiectasis, pulmonary disease	[32]
Cilostazol	DCM, acetic acid	8–15	40–60	50–150	AGG (size: 1.0–4.5 μm)	vasodilator drug to treat vascular claudication	[76]
Telmisartan	EtOH/DCM	12	45	25	Irregular cSMP (m.s.: 740 μm)	drug for hypertension treatment	[70]
HCT	DMF, NMP, DMSO, THF, AC, 2-butanone	15	42	20	AGG, irregular particles	drug to treat hypertension	[33]
Atorvastatin	MeOH	10–18	40–60	25–150	NP, SMP (m.s.: 0.15–0.86 μm)	drug to treat hyper-cholesterolemia	[72]
Piroxicam	DCM	9.7	25	0.05	C	NSAID to treat arthritis, osteoarthritis, spondylitis	[12]
Diclofenac sodium	DMSO	9	40	20	NP (m.s.: 0.14 μm)	NSAID to treat arthritis, osteoarthritis, spondylitis	[46]
Diflunisal	AC, AC/DCM	14–15	35–40	0.02–0.04	C	NSAID for tuberculosis treatment	[11]

Table 1. *Cont.*

Active Compound	Solvent	P [MPa]	T [°C]	C [mg/mL]	Morphology	Applications	Reference
Ibuprofen sodium	EtOH	8–12	35–50	0.0002–0.0004	C	NSAID to treat fever, pains, various inflammations	[84]
Licorice	EtOH	15–20	40	10–14	AGG	thrombin inhibitor with antiulcer, antimicrobial, antidiabetic, hepatoprotective and anticancer activities	[89]
5-fluorouracil	DMSO, DMSO/DCM	15–18	40–50	0.1–0.2	AGG, cSMP (m.s.: 0.22–0.67 μm)	anticancer drug	[67]
DLBS2347	DMSO, EtOH, MeOH, EtAc, AC, DCM	8–20	40–60	Not reported	Film, C, NP-AGG	anticancer drug	[68]
Camptothecin	DMSO	10–25	35–68	1–5	cNP, SMP (m.s.: 0.4–0.9 μm)	anticancer drug	[4]
HCPT	DMSO	10–25	35–68	0.5–5	NP (m.s.: 0.18 μm)	anticancer drug	[3]
Taxol	EtOH	10–25	35–68	2.5–10	NP, MP (m.s.: 0.2–1.9 μm)	anticancer drug	[69]
GBE	EtOH	10–40	35–80	1–5	NP (m.s.: 0.1–0.2 μm)	antioxidant, antifungal and antitumor drug to treat diabetes cardiovascular diseases, cerebral insufficiency, dementia	[5]
Curcumin	EtOH, AC, AC/EtOH	9	40	2–10	AGG	polyphenol with antioxidant and anticancer properties	[80]
Mangiferin	DMSO, AC, NMP, DMSO/AC, DMSO/EtOH, NMP/AC, NMP/EtOH	8–15	40–50	8–14	NP, SMP, cSMP (size: 0.22–1.44 μm)	polyphenol with antioxidant, analgesic, anti-allergic, anticancer properties to treat diabetes, aging, periodontitis, neurodegenerative disease	[66]
Mangiferin	NMP	10–20	35–59	5–59	cSMP, SMP, MP (m.s. 0.56–1.04 μm)	antioxidant	[38]
Curcumin	AC/EtOH	9–12	40	20	Needles	polyphenol	[13]
Resveratrol	MeOH, EtOH, MeOH/DMC, EtOH/DMC	15	40	Not reported	NP, SMP (m.s.: 0.15–0.50 μm)	phenol to treat diabetes, cancer, cardiovascular and neurological disease	[7]
Folic acid	DMSO	15	40	20	AGG	vitamin B9 to prevent neural tube defects in infants, vascular diseases and megaloblastic anemia	[94]

Table 1. *Cont.*

Active Compound	Solvent	P [MPa]	T [°C]	C [mg/mL]	Morphology	Applications	Reference
Lycopene	DCM	7–15	35–45	0.13–0.5	C (m.s.: 10–80 μm)	carotenoid with antioxidant and anticancer properties	[90]
Lutein	EtAc	6.5–9	35–45	0.5–0.9	needles, cNP	carotenoid	[45]
β-carotene	AC/EtOH	8.5	40	4–8	C (m.s. 4–247 μm)	carotenoid with antioxidant and anticancer properties, also used to treat cardiovascular diseases and osteoporosis	[81]
β-carotene	DCM	8–12	40	32–61	C	carotenoid	[95]
β-carotene	DCM	8–20	40	4–8	C	carotenoid	[96]
Rosemary extracts	EtOH	8–12	25–50	Not reported	AGG, cSMP (size: 0.2–1 μm)	antioxidants with antimicrobial, anti-inflammatory and anticancer activities	[78]
Quercetin, Rutin	DMSO	9, 13	40	20	C	flavonoids with antioxidant and anticancer properties, also used to prevent cardiovascular disease	[97]
Quercetin	EtAc	10	35	1.4	needles (0.63 ± 0.06 μm)	flavonoid	[91]
Quercetin	EtOH	8–25	35–65	2–11	C, AGG, needles	flavonoid	[92]
Rutin	DMSO, DMSO/EtOH, DMSO/AC	8–20	40–60	20–85	cSMP, SMP, MP (m.s.: 0.3–1.9 μm)	flavonoid	[1]
Fisetin	EtOH/DCM	10	45	1	rods	flavonoid with antioxidant, neuroprotective, anticancer effects	[31]
Vitexin	DMSO	15–30	40–70	1–2.5	Irregular NP (m.s.: 0.13 μm)	flavonoid to prevent heart disease	[6]

4. SAS Coprecipitation of Active Compounds with Polymeric Carriers

Up to now, the SAS process has been widely exploited to produce composite polymer/active compound systems for various biomedical applications. In particular, composite particles were produced to treat inflammations [8,11,46,65,98,99], infections [17,100–106], asthma and allergies [22,32,44,93], diabetes [35,107,108], hypertension [34,70], and other diseases [39,94,109–113]. Different kinds of active principles, both with synthetic and natural origin, have been incorporated into polymeric particles. In particular, SAS particles loaded with natural active compounds have been often proposed as alternative therapies to conventional ones, e.g., for the prevention and treatment of tumors or cardiovascular diseases [31,49,91,97,114–116]. Carotenoids, phenols, and flavonoids belong to this category of compounds that offer numerous benefits for human health, given their antioxidant, anticancer, antimicrobial, and anti-inflammatory properties.

As occurs for the drug micronization, the coprecipitation of a polymer and an active principle via the SAS process offers many advantages if compared with conventional techniques [12,21–24]. The study of Wu et al. [12] proved the superiority of the SAS process with respect to spray drying in the attainment of polyvinylpyrrolidone (PVP)/piroxicam microparticles. Indeed, the PSD obtained with the SAS technique was narrower than that of the spray-dried particles. Moreover, the dissolution rate of piroxicam released from SAS particles is approximately twice as fast than that of the drug released from the spray-dried particles. In particular, about 2% of pure piroxicam dissolved in 5 min, whereas the percentage of piroxicam released from SAS-processed microparticles and the spray-dried microparticles was about 100% and 55%, respectively [12].

Similarly, Lee et al. [22] prepared inclusion complexes both by the freeze-drying method and the SAS technique. By coprecipitating cetirizine dihydrochloride (an antihistamine drug) with β-cyclodextrin (β-CD), large and irregular crystals were produced by the freeze-drying method, whereas spherical particles were obtained by the SAS technique. In the work of Won et al. [23], the SAS process also showed better performance with respect to the conventional solvent evaporation in the preparation of felodipine-loaded particles based on hydroxypropylmethyl cellulose (HPMC) and poloxamers. In particular, SAS particles proved to be more stable over time, in addition to exhibit a higher drug dissolution rate.

As previously mentioned, polymer/drug composites are produced for various purposes, but the main challenge is to suitably modify the dissolution kinetics of the active principles, aiming for excellent therapies. Depending on the medical application, different drug release kinetics can be required. The choice of the right polymeric carrier is strategic to release the drug at the desired time/speed and/or to a specific site of action. In this context, it was proven that the use of different carriers for SAS coprecipitation leads to different drug releases [46,65]. In particular, when a hydrophilic polymer is used as the carrier, the dissolution of the active principle contained in the SAS composite particles is enhanced. PVP belongs to this category of polymers; indeed, its use allowed to increase the dissolution rate of various poorly-water soluble active compounds [8,9,11,31,33,65,70,81,93,94,97,115–117]. In reverse, the drug release is prolonged using a polymer with a hydrophobic behavior, as occurs, for example, by selecting zein [17,46–49]. Similarly, a sustained or prolonged release of the active compound was observed from particles based on polylactic acid (PLA) and poly (L-lactic acid) (PLLA) [32,67,98,99,111,112,118–121], which, until now, has been mostly employed to deliver anticancer drugs.

In addition, it is also possible to promote a targeted drug release by producing SAS particles based on pH-sensible polymers, i.e., polymers that dissolve at specific pH values. The Eudragit polymers are a striking example [43,44,98,99,104,122].

Two significant examples of improvement of the drug release kinetics by SAS-produced particles are reported in Figure 3. In Figure 3a, the dissolution of a model NSAID (i.e., ketoprofen) was speeded up by selecting PVP as a hydrophilic carrier to ensure a rapid relief against inflammations, such as headache or toothache. In Figure 3b, the release of a model antibiotic (i.e., ampicillin) was

prolonged by producing particles based on zein as a hydrophobic carrier, thus reducing the frequency of administration and the side effects due to antibiotics overuse.

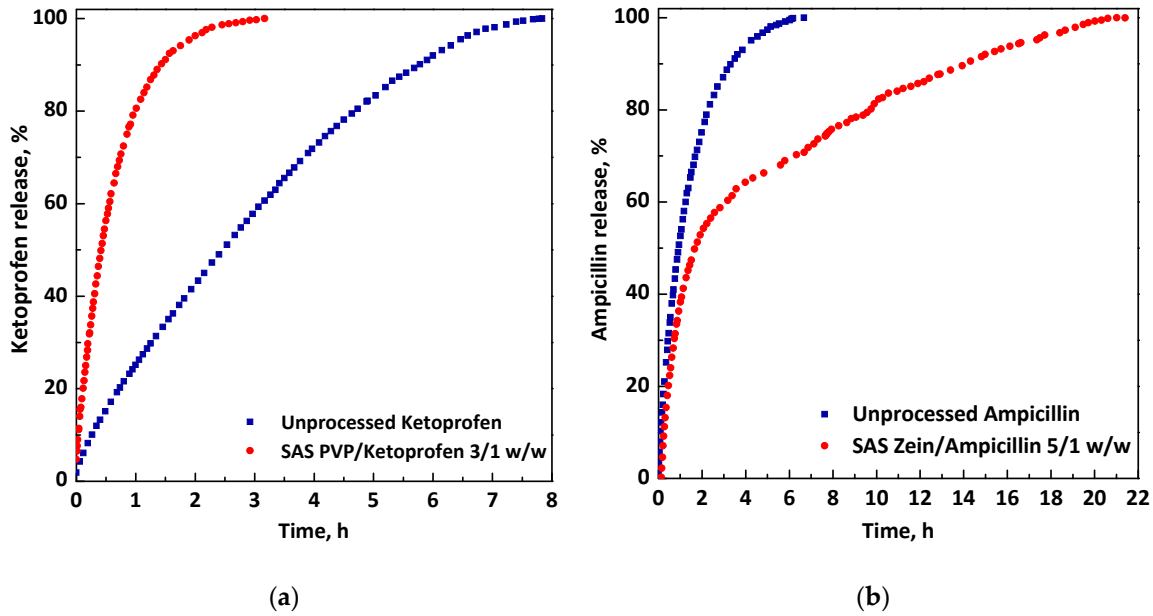

(**a**) (**b**)

Figure 3. Dissolution kinetics of active principles from microparticles obtained through the SAS process: (**a**) Ketoprofen (pure and released from polyvinylpyrrolidone (PVP)); (**b**) ampicillin (pure and released from zein).

However, it is necessary to identify and to use carriers that can be processed by the SAS technique. Up to now, satisfactory results have been reached only with a reduced number of polymers, which are therefore identified as effective carriers for the SAS coprecipitation. PVP is currently the most used polymer and is considered one of the best carriers [8,9,11,31,33,35,65,70,80,81,93,94,97,103,115–117,123] since it is often allowed to obtain regular and spherical composite particles. PVP is followed by PLA [45,108,124] and PLLA [41,67,98,99,111–113,118–121,125–127] that are also suitable carriers often employed. Recently, zein [17,46] is also established as a good polymeric carrier for SAS coprecipitation; moreover, β-CD [22,128] seems to be a promising polymer, but its use has to be further investigated given the very few existing papers. Accurately selecting the solvent and the operating conditions, Eudragit L100-55 also led to the formation of regular composite particles. Therefore, it can be considered a novel carrier more suitable for SAS coprecipitation with respect to the previously tested Eudragits, including Eudragit RS100 and Eudragit RL100 [43,98,99,122]. Eudragit L100-55 is soluble at a pH higher than 5.5, corresponding to the first intestinal tract (duodenum), thus the active compound is protected against the acid gastric fluid; in the meanwhile, the side effects on the gastric tract are also avoided. Eudragit L100-55 allowed reaching a controlled release of NSAIDs, antibiotics, and bronchodilator drugs from SAS microspheres [44,104]. Until now, the SAS coprecipitation was attempted using other kinds of polymers, such as polyethylene glycol (PEG) [35,106,129,130], poly(lactide-co-glycolide) (PLGA) [36,37,109], ethyl cellulose (EC) [91,100–102,105], HPMC [34,39,42,70,107], and poly(hydroxybutyrate-co-hydroxyvalerate (PHBV) [95,96,131–135]. However, the use of these carriers must be further investigated, by changing the selected solvents or/and the operating conditions, because the morphology of the polymer/drug precipitated powder is not yet satisfactory.

Indeed, in addition to respecting the essential prerequisites of the SAS technique, it has to be considered that the SAS coprecipitation seems to be effective when composite microspheres are obtained, i.e., microparticles consisting of a polymeric matrix in which the drug is homogeneously dispersed [46]. In this case, in the meanwhile that the liquid solution is fed to the precipitator, the liquid

jet break-up and the subsequent atomization quickly occur and prevail with respect to the surface tension vanishing. As a consequence, the polymer and the active compound are entrapped in the same droplet, which behaves as an isolated reactor. The droplet drying by $scCO_2$ leads to the attainment of the composite microsphere, as represented in Figure 4.

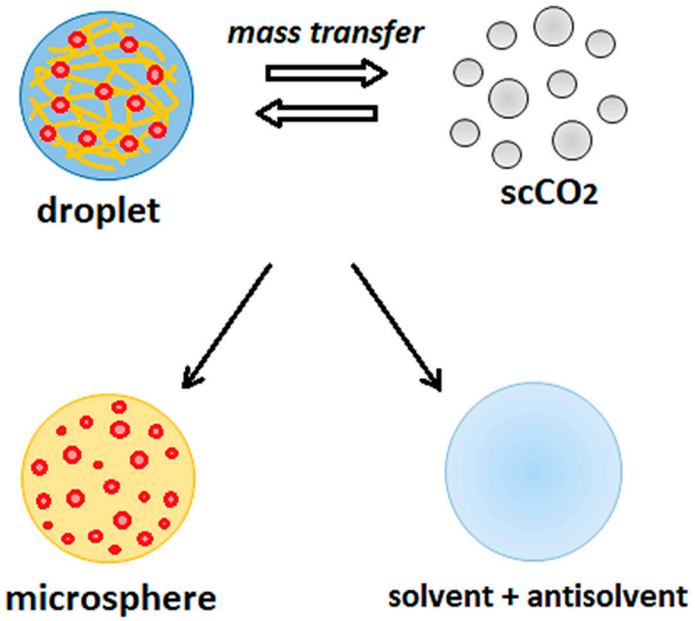

Figure 4. Mechanism of formation of a polymer/active compound microsphere by the SAS technique.

On the contrary, when nanoparticles precipitate, the coprecipitation fails at least in part. In particular, nanoparticles are formed when the surface tension vanishing is very fast, and the gas mixing prevails on the breakage of the liquid jet. Consequently, no droplets are formed and the precipitation of nanoparticles occurs by gas-to-particles nucleation and growth. In this case, a sort of physical mixture at the nanometric level is obtained, i.e., polymer nanoparticles mixed with nanoparticles of the active compound. In addition, in the case of the sub-microparticles, a specific portion of the recovered powder consists of the polymer and the drug precipitated together, but with an irregular distribution of the two materials. Hence, the achievement of an effective polymer/active compound coprecipitation seems to be strongly influenced by the size and the morphology of the particles produced, as well as by their shape. Indeed, the coprecipitation fails also in the case of the attainment of crystals, which occurs by operating in the miscibility gap between the solvent and the antisolvent, where the two compounds tend to precipitate separately, resulting in polymer crystals and drug crystals.

This correlation between a successful coprecipitation and the morphology/size of particles was proved in the study of Franco et al. [46] employing the dissolution tests. In particular, using zein as the carrier and diclofenac sodium as the model drug, it was observed that, increasing the polymer/drug ratio, the particles' diameter increased, whereas the release of the active compound was further slowed down. Moreover, as the particle size decreased, the burst-like effect, i.e., the dissolution of the drug near/on the particles' surface, which, therefore, dissolve as quickly as the unprocessed drug increased.

Several papers showed that the selection of a proper carrier could force even the morphology of active principles that cannot be processed alone by the SAS technique [5,8–13,44]. Moreover, the entrapment of the active compound into the amorphous polymeric matrix can also favor the inhibition of the drug recrystallization [136].

Nevertheless, it has to be taken into account that the presence of the active compound can modify the polymer processability even if, under the selected process conditions, the carrier can be micronized alone in well-defined particles [44]. This influence may be a consequence both of

an interaction between the polymer and the drug, but usually, it is due to the presence of solutes (polymer and/or active principle) that can alter the high-pressure VLEs. Therefore, the critical point of the solvent/polymer/drug/antisolvent quaternary mixture can shift with respect to that of the solvent/scCO_2 binary mixture [82,83]. Each compound (i.e., carrier and drug) has a different influence on VLEs, which might be negligible or not; thus, the morphology of the precipitated composites also depends on this factor.

In the case of the coprecipitation, it is evident that the polymer/drug ratio plays a crucial role in the attainment of composite particles. Moreover, the polymer content strongly affects the dissolution rate; in general, the release of the active compound is mostly modified by increasing the polymer/drug ratio [23,41,46,99,110,117,119].

Aiming to obtain spherical microspheres that guarantee an effective coprecipitation, in some cases, it is not possible to reduce the amount of polymer in the composite particles beyond a specific value [97,123]. In particular, a high polymer content in the pharmaceutical formulations can be a limitation of the SAS coprecipitation when some carriers are employed. Among these, up to now, the use of Eudragit L100-55 allowed producing well-defined microparticles only at polymer/drug ratios equal to 20/1 and 10/1 *w*/*w* [44,104]. Similarly, in the studies of Chhouk et al. [123] and Ozkan et al. [97], polymer/active compound ratios equal to 30/1 and 20/1 *w*/*w* were indicated as optimal for the production of PVP/curcumin and PVP/quercetin particles, respectively. However, this drawback was found only in these few cases using PVP as the carrier. Alternatively, a high amount of polymer in the SAS coprecipitated powders can be avoided by selecting β-CD.

In general, cyclodextrins (CDs) are characterized by a hydrophilic external surface, which makes them very soluble in water, and a hydrophobic internal cavity, in which various molecules can be incorporated to form guest/host inclusion complexes by non-covalent interactions. The production of CDs-based inclusion complexes by the SAS technique has been exploited to mask the bitter taste and/or to increase the dissolution of various active compounds, such as antioxidants [114,128,137,138], antihistamine drugs [22], antibiotics [139], and others [140]. In these papers, hydroxypropyl-β-cyclodextrin (HP-β-CD) [114,137–140] is mainly employed, followed by β-CD [22,128]. In particular, from the few available studies, β-CD seems to be a more suitable carrier for the SAS process with respect to H-β-CD, since composite particles of regular morphology and size were successfully produced only with β-CD. In addition, inclusion complexes are generally formed by using a low polymer content, i.e., from molar ratio polymer/drug equal to 3/1 up to 1/2 mol/mol. Therefore, the application of β-CD may be a useful tool to reduce the amount of polymeric carrier in the SAS-prepared composite particles significantly, when a rapid drug release is desired.

In addition to the polymer/active compound ratio, other parameters influence the morphology and size of composite particles, mainly the pressure and the overall concentration of solutes in the liquid solution [8,9,44,65,80,81,93,94,97,110,117]. If the pressure is too high, the disappearance of the surface tension prevails over the breakage of the liquid jet, and the coprecipitation partly fails with the formation of nanoparticles, as previously mentioned. This failure also occurs if the pressure is too low and below the MCP, hence the operating point lies in the biphasic region, resulting in the precipitation of crystals or aggregates; even, the liquid can be recovered in the precipitator. Regarding the total concentration, undoubtedly, the upper limit is represented by the solubility of the solutes in the selected solvent. Nanoparticles or coalescent particles often precipitate when the concentration of solutes is too low, because of the fast vanishing of the surface tension and the low viscosity of the injected solution, not allowing the generation of well-defined droplets. Moreover, in the case of a low concentration in the solution, the content of the polymeric carrier, which acts as a microsphere-forming agent, is not enough to force the morphology of the composite system and to trap the active compound into the polymeric matrix. On the contrary, if the total concentration is too high, aggregates or even crystals can be obtained due to the influence that solutes may have on VLEs, as explained above.

In some cases, the variation of the temperature can favor the attainment of well-separated microparticles, as occurs with zein [17,46]. As demonstrated in the study of Franco et al. [17],

by coprecipitating ampicillin (a model antibiotic) and zein at a fixed pressure (90 bar) and total concentration (50 mg/mL), polymer/drug 20/1 *w*/*w* sub-microparticles (mean size: 0.36 ± 0.30 μm) were produced working at 40 °C. Instead, spherical microparticles with a mean size in the range 19–9 μm were obtained at 50 °C, also managing to reduce the ampicillin/zein ratio up to 5/1 *w*/*w*. The morphology and shape of zein-based particles prepared by the SAS process are also definitely better than aggregates and irregular or collapsed particles obtained up to now with the techniques commonly used in the pharmaceutical field, namely spray freeze-drying and spray-drying [141–143].

A similar trend to that shown in the study of Franco et al. [17] was also reported in the paper of Montes et al. [99] since the dimensions of ibuprofen-loaded particles produced using PLLA or Eudragit L100 increased by increasing the temperature. Instead, Kalogiannis et al. [59] and Patomchaiviwat et al. [119] observed a rise in the degree of coalescence of the PLLA-based particles by increasing the temperature up to 50 °C, probably due to the PLLA plasticization. Indeed, it is well known that the glass transition temperature (T_g) of a polymer can be depressed in the presence of the $scCO_2$, because of its absorption into the polymeric matrix that leads to a weakening of the intramolecular and intermolecular attractions between the polymeric segments [144–146]. Therefore, the polymer T_g decreases in proportion to the amount of $scCO_2$ that the polymer is able to absorb. The CO_2 absorption and, consequently, its plasticizing effect in the presence of semicrystalline polymers also depends on the operating temperature, which influences the $scCO_2$ properties.

A glaring gap emerged from the SAS literature: Up to now, the use of polymeric blends has been employed to produce drug delivery systems in very few papers [23,37,40,41]. Polymer blends can be exploited to tune the drug release as desired, by modulating the ratio between the hydrophilic and hydrophobic polymers that constitute the microparticles. In addition, they are useful to improve other features of the final product, such as mechanical properties and moisture absorption. For example, the very hydrophilic PVP can induce a hygroscopic effect, which could lead to low stability over time and high water uptake in the produced composite powders. This critical issue can be overcome by introducing hydrophobic polymers in the formulation, thus increasing the particles' resistance to humidity. Lee et al. [37] selected PLGA and PLLA to produce microspheres loaded with bupivacaine HCl, a local anesthetic drug generally administered by parental route for the regional anaesthesia, i.e., the local pain control. Various PLGA/PLLA mass ratios were investigated, as well as the use of PLLA at two different molecular weights (MW 2000 or 50,000). It was proved that the release of bupivacaine HCl from particles obtained by SAS depends on the PLGA/PLLA ratio and on the molecular weight of PLLA. In particular, by increasing the PLGA content, the drug dissolution rate increased, until having a rapid release (in about 4 h) when only PLGA was used.

On the contrary, both molecular weight PLLA prolonged the bupivacaine dissolution, but a slower drug release with a lower burst-like effect was achieved when the lower molecular weight PLLA (MW 2000) was employed. These results are partly also since the particles' morphology improved as the PLGA content decreased. Amphiphilic block copolymers, obtained by combining hydrophilic and hydrophobic polymeric segments, can also be employed to deliver active compounds. For example, in the paper of Jung et al. [41], PLLA, methoxy poly-(ethylene glycol)-b-poly(L-lactide) (mPEG-PLLA) block copolymers or PLLA/PEG blends were chosen as carriers for controlled delivery of leuprolide acetate. The last-mentioned one is a non-steroidal antiandrogen drug used to treat prostate and breast cancers and endometriosis, which is usually administered via the parenteral route, being not orally bioavailable. However, leuprolide-based therapies require long-term daily injections and frequent administrations because this drug is very water-soluble and it has a short half-life when administrated via the parenteral route. The mPEG-PLLA diblock copolymers were synthesized by ring opening polymerization of L-lactide in the presence of PEG chain lengths. The effect of the mPEG block length, the PEG/PLLA blending, and the polymer/drug ratio on the leuprolide acetate release were investigated. A dichloromethane/methanol 1/1 *v*/*v* mixture was used for the SAS coprecipitation, and in all the investigated conditions, spherical microparticles were produced. It was observed that the

mean diameter of PLLA-based microparticles was higher than the one of microparticles prepared using mPEG-PLLA.

Moreover, an increase in the mean particle size was noted as the PEG block length increased in the mPEG-PLLA diblock copolymer. The drug entrapment efficiency was not significantly influenced by the mPEG block length in mPEG-PLLA, the blending of PLLA and PEG, as well as the polymer/drug ratio. However, these factors influence the release of leuprolide acetate from SAS microparticles. Indeed, the drug dissolution rate increased by increasing the PEG block length in the mPEG-PLLA. Microparticles based on PEG/PLLA blends showed a faster drug release with respect to the mPEG-PLLA copolymer containing an equal mass ratio PEG/PLLA. Concerning the effect of the polymer/drug ratio, a higher amount of mPEG-PLLA allowed a slower drug release rate.

Recently, some changes to the SAS process have been suggested [13,47]. In particular, Matos et al. [13] proposed a single-step coprecipitation and coating by using the supercritical antisolvent. A SAS coprecipitation of PVP/curcumin particles was attempted to coat the surface of different polymers, namely microcrystalline cellulose (MCC) (size of crystals/irregular particles: 175 μm), corn starch (size: 15 μm), or lactose (size: <5 μm). Briefly, before starting the experiment, irregular particles/crystals of MCC, starch, or lactose were located into the precipitator; then, the solution containing PVP and curcumin is injected and, because of the antisolvent effect of the $scCO_2$, composite particles precipitated onto the different polymers used as support. During the single-step coprecipitation and coating, the stirring into the precipitator ensured a homogeneous coating onto the polymer surface. However, a proper morphology of the final product was not guaranteed, since it strongly depends on the shape of the polymeric supports initially charged into the precipitator. Moreover, from the release tests, it can be noted that only about 10% of the unprocessed curcumin dissolved in 60 min. In contrast, the drug released from PVP-based particles precipitated by a conventional SAS coprecipitation (i.e., without other polymeric supports) already reached more than 95% of dissolution in 5 min. The dissolution of curcumin did not show a further improvement when PVP/curcumin particles were precipitated onto the polymeric supports. Instead, Liu et al. [47] attempted to incorporate an anticancer compound, namely 10-hydroxycamptothecin (HCPT), into zein-based particles. By coprecipitating the polymer and the drug through the SAS technique, rods-like crystals and drug nanoparticles were obtained. These results suggest that coprecipitation did not occur because the polymer and the drug precipitated separately and not in the form of composite microspheres. An unsatisfactory morphology was also achieved using the built-in ultrasonic dialysis process (BUDP), which couples the ultrasonic emulsification with the dialysis technologies [147]. Then, the authors combined the supercritical process with the BUDP by dispersing the SAS coprecipitated zein/HCPT powders into an ethanol/water mixture, which was used as the dialysis solution for BUDP. In this way, well-defined zein/HCPT microspheres were produced, also prolonging the drug release. However, nowadays, aiming at the process intensification, the use of a multistage-procedure is not the best option, both in terms of costs and of process times.

A summary of the polymer/active compound composites produced by the SAS technique for medical purposes is reported in Table 2. The polymeric carriers and the active principles processed were indicated, as well as the main process parameters, including the liquid solvent used, the pressure (P), the temperature (T), and the overall concentration of solutes (polymer + drug) in the liquid solution (C_{tot}). The morphology and the dimensions of SAS-obtained samples are also specified. In particular, the literature results are listed in Table 2, firstly reporting the polymers that revealed to be the most used and the most suitable for the SAS technique.

Table 2. An overview of the polymer/active compound composites obtained by the SAS technique. C: Crystals; m.s.: Mean size; c: Coalescent; NP: Nanoparticles; SMP: Sub-microparticles; MP: Microparticles; EMP: Expanded microparticles (*balloons*); AGG: Aggregates; AC: Acetone; CHF: Chloroform; DCM: Dichloromethane; DMF: Dimethylformamide; DMSO: Dimethylsulfoxide; EtOH: Ethanol; EtAc: Ethyl acetate; MeOH: Methanol; NMP: N-methyl-2-pyrrolidone; THF: Tetrahydrofuran; PVP: Poly(vinylpyrrolidone; MCC: Microcrystalline cellulose; β-CD: β-Cyclodextrin; HP-β-CD: Hydroxypropyl-β-cyclodextrin; PLA: Polylactic acid; PCL: Poly(ε-caprolactone); PLGA: Poly(lactide-co-glycolide); PLLA: Poly(L-lactic acid); PEG: Poly-ethylene glycol; mPEG-PLLA: Methoxy poly(ethylene glycol)-b-poly(L-lactide); HPMC: Hydroxypropylmethyl cellulose; HPC: Hydroxypropyl cellulose; HCO-60: Polyoxyethylene (60) hydrogenated castor oil; CAP: Cellulose acetate phthalate; PHBV: Poly(hydroxybutirate-co-hydroxyvalerate); PVM/MA: Polymer poly(methyl vinyl ether-co-maleic anhydride); PMMA: Poly(methyl methacrylate; HCT: Hydrochlorothiazide; HCPT: 10-Hydroxycamptothecin; 17α-MT: 17α-Methyltestosterone; PZA: Pyrazinamide).

Polymeric Carrier	Active Compound	Solvent	P [MPa]	T [°C]	C_{tot} [mg/mL]	Morphology	Reference
PVP	Cefuroxime axetil	MeOH	7–20	35–50	50–150	cMP, MP (m.s. 1.88–3.97 μm)	[103]
	Ezetimibe	EtOH	15	40	25	NP (m.s. 0.21–0.23 μm)	[110]
	Dexamethasone, prednisolone, budesonide	EtOH	9–15	40	10–30	Dexamethasone MP (m.s. 1.82–2.51 μm), prednisolone MP (m.s. 1.96–3.03 μm), budesonide MP (m.s. 3.06–3.58 μm)	[93]
	Telmisartan	EtOH/DCM	12	45	25	SMP, MP (m.s. 0.38–0.60 μm)	[70]
	HCT	DMSO, DMSO/AC	8.6–19	30–40	10–30	NP (0.05–0.21 μm)	[33]
	Oxeglitazar	EtOH/CHF	8	35	30	C	[35]
	Nimesulide	DMSO	9–15	35–45	20–35	AGG or MP (m.s. 1.67–4.04 μm)	[8]
	Piroxicam	DCM	9.7	25	0.05	MP (0.1–5.0 μm)	[12]
	Ketoprofen	DMSO	9–15	40	10–50	MP (m.s. 2.41–3.81 μm)	[65]
	Diflunisal	AC/DCM	12–14	35	18–36	cNP, cMP (size: 0.4–8.1 μm)	[11]
	Folic Acid	DMSO	9–15	35–40	20–40	NP 0.05–0.20, SMP, MP (m.s. 0.30–3.80 μm)	[94]
	α-tocopherol, menadione	DMSO	9–15	35–50	20–60	α-tocopherol MP (m.s. 1.80–4.08 μm), menadione MP (m.s. 2.64–5.09 μm)	[9]
	Quercetin, rutin	DMSO	9	40–50	20–40	Quercetin MP (m.s. 0.47–9.52 μm), rutin MP (m.s. 0.84–8.17 μm)	[97]
	Fisetin	EtOH/DCM	10	45	Not reported	NP, SMP (0.08–0.72 μm)	[31]
	Chrysin	AC/EtOH	12	40	1–3	SMP (m.s. 0.27–0.96 μm)	[116]
	β-carotene	AC/EtOH	8.5–10	40	5–7	NPs (m.s. 0.25– μm), MP (m.s. 0.81–2.43 μm)	[81]
	Anthocyanins	EtOH	10	40	Not reported	C, AGG	[21]
	Curcuma	AC/EtOH	15–21	35–45	2–10	NP (m.s.0.11–0.21 μm)	[115]

Table 2. *Cont.*

Polymeric Carrier	Active Compound	Solvent	P [MPa]	T [°C]	C_{tot} [mg/mL]	Morphology	Reference
PVP and MCC, starch or lactose	Curcumin	AC/EtOH	8–12	40–60	1	cSMP, SMP (size <1 μm)	[117]
	Curcumin	AC/EtOH	10–20	30–50	1–10	NP, SMP (m.s. 0.03–0.34 μm)	[123]
	Curcumin	EtOH, AC/EtOH	2–12	35–50	5–20	AGG, NP or SMP (m.s. 0.05–0.33 μm)	[80]
	Curcumin	AC/EtOH	9–12	40	20	irregular particles/C of MCC (size: 175 μm), starch (size: 15 μm) or lactose (size <5 μm) coated with PVP/curcumin particles	[13]
PLA	Budesonide	DCM	8.6	40	14	MP (1.26 μm)	[32]
	Cholesterol	DCM	9	45	10, 46	MP (1.70 μm), C (8.0 μm)	[124]
	Insulin	DMSO/ DCM	8.5–13	20–38	1	MP (0.50–2.0 μm)	[108]
PLA/PCL	Lutein	EtAc	10	17	21.8–22.2	cMP (m.s. 1.0–10.0 μm)	[45]
	17α-MT	DCM	8	40	0.01	MP (23.0–54.0 μm)	[40]
	Ibuprofen	DCM	12–20	40–50	5–10	MP (0.93–1.97 μm)	[99]
	Naproxen	DCM	10–20	40–50	5–8	MP (0.56–1.43 μm)	[98]
PLLA	Amoxicillin	DMSO/ DCM	10–20	29–50	2–9	MP	[125]
	Rifampicin	DCM	14–21	33–50	10–30	MP (m.s. 3.26–30.53 μm)	[119]
	Azacytidine	DMSO/ DCM	11	40	19	C+MP (2.0 μm)	[111]
	Leuprolide acetate	DCM/ MeOH	13	35	11–12	MP	[41]
	Zidovudine	EtOH/ DCM	8.5–13.5	45	0.2	Filaments	[120]
	5-fluorouracil	EtOH/ DCM	12	33	4	MP (0.98 μm)	[112]
	5-fluorouracil	DMSO/DCM	12–25	35–50	0.1–0.2	AGG	[67]
	HCPT	EtOH/DCM	7.5–12	30–40	1–9	MP (0.57–1.37 μm)	[118]
	Paclitaxel	DCM, DCM/ DMSO, DCM/EtOH	8–14	30–45	7–14	MP (0.83–1.43 μm)	[126]
	Tamoxifen citrate	DCM	13	38	13.5	MP	[113]

Table 2. *Cont.*

Polymeric Carrier	Active Compound	Solvent	P [MPa]	T [°C]	C_{tot} [mg/mL]	Morphology	Reference
zein	Astaxanthin	DCM/AC	8–12	30–42	5–12	Irregular MP (size: 0.6–2.0 μm)	[127]
	Gefitinib	EtOH/ DCM	9–12	33–48	6–13	MP (size: 1.1–3.8 μm)	[121]
	Lutein	AC/ DMSO	10	32–45	10–20	SMP (m.s. 0.20–0.36 μm)	[49]
	riboflavin, δ-tocopherol, β-carotenein	EtOH	16	40	22–270	EMP, MP (m.s. 8–18 μm)	[148]
	HCPT	DMSO, DMSO/EtOH	8–14	35–45	6–21	Rods, C+NP	[47]
	Lysozyme	EtOH/H_2O	10	40	0.05	Collapsed MP/EMP with internal porosity (size up to 50 μm	[48]
	Diclofenac sodium	DMSO	9	40	30–50	SMP, MP (m.s. 0.42–1.3 μm)	[46]
	Amoxicillin, Ampicillin	DMSO	9	40–50	50	SMP, MP (m.s.: 0.65–12.0 μm for amoxicillin, 0.36–19 μm for ampicillin)	[17]
β-CD	Lycopene	DMF	10–14	40–50	1	NP (m.s. 0.04–0.12 μm)	[128]
	Cetirizine dihydrochloride	DMSO	15	35	10–24	SMP-MP (0.29–4.16 μm)	[22]
	Apigenin	DMF	10–25	35–65	67–402	needles + cSMP (m.s. 0.4 μm)	[114]
H-β-CD	Simvastatin	DCM/EtOH	12	40	Not reported	AGG	[140]
	Tosufloxacin tosylate	DCM/DMF	8–16	35–55	Not reported	C	[139]
	Resveratrol	EtOH	12	40	0.03	AGG/cNP	[137]
	Baicalein	AC/EtOH	8–14	35–50	Not reported	C, AGG (m.s. 0.3–1.0 μm)	[138]
Eudragit RS100, Eudragit RL100	Acetazolamide	AC	5.7–9	27–40	15–24	Needles + cMP, AGG	[43]
Eudragit L100	Ellagic acid	NMP	15	40	20	MP+C	[122]
	Ibuprofen	AC	12–20	40, 50	5–10	NP (0.08–0.21 μm), SMP (51 μm)	[99]
	Naproxen	EtOH	10–20	40–50	5–8	NP (0.08–0.15 μm) SMP (0.31 μm)	[98]
Eudragit L100–55	Ampicillin	DMSO	9–10	40	20–40	cMP, MP (m.s.: 1.5–2.5 μm	[104]

Table 2. *Cont.*

Polymeric Carrier	Active Compound	Solvent	P [MPa]	T [°C]	C_{tot} [mg/mL]	Morphology	Reference
PLGA	Diclofenac sodium, theophylline	DMSO	9–15	40	20–50	C, EMP, cMP, MP (m.s.: 1.5–2.9 μm for diclofenac, 1.6–6.8 μm for theophylline)	[44]
	5-Fluoracil	Acetone, DCM/ methanol	11	36, 36–45	6, 6–30	Film, cMP	[109]
	Hydrocortisone	AC, MeOH/ DCM	9	33	20	C	[36]
PLGA, PLGA/PLLA	Bupivacaine HCl	EtOH/ DCM	8	40	Not reported	MP + Fibers (5.56–7.07 μm), MP (4.39–10.9 μm)	[37]
PEG	β-carotene, Lutein	DCM	8–10	15	13–17	MP and C for β-carotene, AGG and irregular cMP for lutein	[129]
	Carotene	DCM	16	35–50	6	C+cMP (m.s. 1–10 μm)	[149]
	Emodin	DCM/ MeOH	8–20	35–50	1	C (m.s. 3–20μm)	[130]
	Itraconazole	AC	19	40	2	C+ MP (m.s. 3 μm)	[106]
	Oxeglitazar	CHF	8	35	30	C	[35]
mPEG/PLLA	Leuprolide acetate	DCM/ MeOH	13	35, 15	11–12	MP (m.s. 2.86–5.63 μm)	[41]
Ethyl cellulose	Amoxicillin	DMSO/ DCM	10–25	35–65	10	cMP (m.s. 0.23–2.66 μm)	[102]
	Ampicillin	DMSO/ DCM	10–25	35–55	11	cMP (m.s. 1.0–3.0 μm)	[100]
	Amoxicillin	DMSO/ DCM	10–15	35–50	23–24	AGG, MP	[101]
	Quercetin	EtAc	10	35	1.4	cNP, cSMP (m.s. 0.18–0.34 μm)	[91]
	Rifampicin	EtAc, EtAc/ DMSO	10	35–60	13–15	NP+C NP (m.s. 0.19–0.23 μm)	[105]
PMC	Insulin	DMSO/AC	12	32	2, 4–7	NP (0.14 μm), SMP (m.s. 0.27–0.34 μm)	[107]
	Itraconazole	EtOH/ DCM	8–15	45–60	Not reported	C+NP/cSMP (size: 0.1–0.5 μm)	[42]
	Lercanidipine	EtOH/ DCM	15	40	50	NP, SMP (m.s. 0.22–0.44 μm)	[34]
	Megestrol acetate	EtOH/ DCM	15	40	52	NP, SMP (m.s. 0.14–0.50 μm)	[39]

Table 2. *Cont.*

Polymeric Carrier	Active Compound	Solvent	P [MPa]	T [°C]	C_{tot} [mg/mL]	Morphology	Reference
HPMC/poloxamers/ HCO-60	Telmisartan	EtOH/ DCM	12	45	25	SMP (m.s. 0.45–0.50 μm)	[70]
	Felodipine	EtOH/ DCM	10	45	Not reported	cNP/cSMP (m.s. 0.20–0.25 μm)	[23]
Poloxamers	Oxeglitazar	DMC, EtOH/CHF	8	35	23	C	[35]
	Rosemary extracts	EtOH	10	50	Not reported	cSMP	[78]
PHBV	Astaxanthin	AC	8–12	35–40	6	cMP	[150]
	Quercetin	AC	10	40	0.03–0.2	cMP (1 μm)	[151]
	β-carotene	DCM	8	40	21–48	Irregular cMP, EMP, AGG	[135]
	β-carotene	DCM	8–20	40	32–61	Not reported	[96]
	Astaxanthin	DCM	8–10	35	5–10	SMP (m.s. 0.22–0.40 μm)	[131]
	Bixin	DCM	8–10	35–40	1.4–20.4	SMP (m.s. 0.20–0.55 μm)	[132]
	Grape seed extract	DCM	8–12	35–45	27–40	SMP (m.s. 0.62–0.72 μm)	[133]
	Pink pepper extract	DCM	8–12.5	35–55	30	cSMP, MP (m.s. 0.39–25.4 μm)	[134]
CAP	Quercetin	AC	9	40	20	NP+C	[152]
	Mangiferin	AC/DMSO	18	50	8–26	cSMP (m.s. 0.25–0.41 μm)	[153]
HPC	Ezetimibe	EtOH	12–18	40–50	10–25, 50–100	NP (m.s. 0.15–0.24 μm) SMP, MP (m.s. 0.33–0.91 μm)	[110]
Lactose	sulfamethoxazole	AC	10	35	88	AGG	[74]
	Rifampicin	MeOH	12.4	40	1–5	cMP < 8 μm	[154]
Lecithin/α-tocopherol	Lycopene	DMF	8–12	35	20–30	C	[155]
PVM/MA	Gentamicin	AC	10	25	140	NP, MP (m.s. 0.05–0.93 μm)	[156]
PMMA	ivermectin	AC	9–11	40–60	33	cNP, NP (m.s. 0.05–0.17 μm)	[157]
Urea, thiourea or PZA	5-fluorouracil	MeOH	7–15	40	4–8	C	[158]
L-arginine	glimepiride	DCM/EtOH	12	60	7	C (m.s. 5–79 μm)	[24]
Stearic acid	hesperidin	DMSO	8–20	35–45	75	NP-SMP (m.s. 0.15–0.39 μm)	[159]
Saccharin	Indomethacin	EtOH, MeOH, EtAc	8.4–9	50	Not reported	C	[160]

5. Conclusions

This review is focused on the application of the SAS technique in the biomedical field. In this context, the micronization and coprecipitation by the supercritical antisolvent have been proposed for several purposes. Regarding the production of composite particles, the opportunity of modulating the drug release by choosing a carrier based on the required therapy is particularly impressive. In this way, it is possible to release the active principle to a specific site of action and/or at the desired dissolution rate, therefore reducing the side effects caused by drug overdoses and improving the patient's compliance. However, to date, few polymers can be defined as valid for a successful SAS coprecipitation in the form of microspheres, including PVP, PLA, PLLA, zein, and Eudragit L100-55. From the very few conducted studies, β-CD also seems a promising SAS carrier, but its use has yet to be deeply investigated. The main challenge is, therefore, to identify new polymeric carriers suitable for the SAS coprecipitation, in order to develop novel polymer/active compound systems and overcome the main issues still existing in the biomedical field. A key role may be played by the use of polymeric blends, which is still practically unexplored with regard to the SAS technique. Maintaining the microparticles' morphology and varying the content of hydrophobic and hydrophilic polymers, the release can be tuned according to the specific application. Anyway, the use of the SAS technique in the biomedical field is strategic to produce composite systems without residues of solvents that are toxic for human health and to produce particles in a controlled manner with a narrow PSD.

Author Contributions: Conceptualization, P.F. and I.D.M.; methodology, P.F.; writing—original draft preparation, P.F.; writing—review and editing, I.D.M.; supervision, I.D.M. All authors have read and agreed to the submitted version of the manuscript.

Funding: This research received no external funding.

Conflicts of Interest: The authors declare no conflict of interest.

References

1. Montes, A.; Wehner, L.; Pereyra, C.; De La Ossa, E.M. Precipitation of submicron particles of rutin using supercritical antisolvent process. *J. Supercrit. Fluids* **2016**, *118*, 1–10. [CrossRef]
2. Chen, Y.-M.; Tang, M.; Chen, Y.-P. Recrystallization and micronization of sulfathiazole by applying the supercritical antisolvent technology. *Chem. Eng. J.* **2010**, *165*, 358–364. [CrossRef]
3. Zhao, X.; Zu, Y.; Jiang, R.; Wang, Y.; Li, Y.; Li, Q.; Zhao, D.; Zu, B.; Zhang, B.; Sun, Z. Preparation and physicochemical properties of 10-hydroxycamptothecin (HCPT) nanoparticles by supercritical antisolvent (SAS) process. *Int. J. Mol. Sci.* **2011**, *12*, 2678–2691. [CrossRef] [PubMed]
4. Zhao, X.; Zu, Y.; Li, Q.; Wang, M.; Zu, B.; Zhang, X.; Jiang, R.; Zu, C. Preparation and characterization of camptothecin powder micronized by a supercritical antisolvent (SAS) process. *J. Supercrit. Fluids* **2010**, *51*, 412–419. [CrossRef]
5. Zhao, C.; Wang, L.; Zu, Y.; Li, C.; Liu, S.; Yang, L.; Zhao, X.; Zu, B. Micronization of Ginkgo biloba extract using supercritical antisolvent process. *Powder Technol.* **2011**, *209*, 73–80. [CrossRef]
6. Zu, Y.; Zhang, Q.; Zhao, X.; Wang, D.; Li, W.; Sui, X.; Zhang, Y.; Jiang, S.; Wang, Q.; Gu, C. Preparation and characterization of vitexin powder micronized by a supercritical antisolvent (SAS) process. *Powder Technol.* **2012**, *228*, 47–55. [CrossRef]
7. Ha, E.-S.; Park, H.; Lee, S.-K.; Sim, W.-Y.; Jeong, J.-S.; Baek, I.-h.; Kim, M.-S. Pure Trans-Resveratrol Nanoparticles Prepared by A Supercritical Antisolvent Process Using Alcohol and Dichloromethane Mixtures: Effect of Particle Size on Dissolution and Bioavailability in Rats. *Antioxidants* **2020**, *9*, 342. [CrossRef]
8. Prosapio, V.; Reverchon, E.; De Marco, I. Formation of PVP/nimesulide microspheres by supercritical antisolvent coprecipitation. *J. Supercrit. Fluids* **2016**, *118*, 19–26. [CrossRef]
9. Prosapio, V.; Reverchon, E.; De Marco, I. Incorporation of liposoluble vitamins within PVP microparticles using supercritical antisolvent precipitation. *J. CO2 Util.* **2017**, *19*, 230–237. [CrossRef]
10. Zhang, H.-X.; Wang, J.-X.; Zhang, Z.-B.; Le, Y.; Shen, Z.-G.; Chen, J.-F. Micronization of atorvastatin calcium by antisolvent precipitation process. *Int. J. Pharm.* **2009**, *374*, 106–113. [CrossRef]

11. Zahran, F.; Cabañas, A.; Cheda, J.A.R.; Renuncio, J.A.R.; Pando, C. Dissolution rate enhancement of the anti-inflammatory drug diflunisal by coprecipitation with a biocompatible polymer using carbon dioxide as a supercritical fluid antisolvent. *J. Supercrit. Fluids* **2014**, *88*, 56–65. [CrossRef]
12. Wu, K.; Li, J.; Wang, W.; Winstead, D.A. Formation and characterization of solid dispersions of piroxicam and polyvinylpyrrolidone using spray drying and precipitation with compressed antisolvent. *J. Pharm. Sci.* **2009**, *98*, 2422–2431. [CrossRef] [PubMed]
13. Matos, R.L.; Lu, T.; Leeke, G.; Prosapio, V.; McConville, C.; Ingram, A. Single-step coprecipitation and coating to prepare curcumin formulations by supercritical fluid technology. *J. Supercrit. Fluids* **2020**, *159*, 104758. [CrossRef]
14. Stebbins, N.D.; Ouimet, M.A.; Uhrich, K.E. Antibiotic-containing polymers for localized, sustained drug delivery. *Adv. Drug Del. Rev.* **2014**, *78*, 77–87. [CrossRef] [PubMed]
15. Gürsel, İ.; Korkusuz, F.; Türesin, F.; Alaeddinoğlu, N.G.; Hasırcı, V. In vivo application of biodegradable controlled antibiotic release systems for the treatment of implant-related osteomyelitis. *Biomaterials* **2000**, *22*, 73–80. [CrossRef]
16. Liu, Z.; Lu, W.; Qian, L.; Zhang, X.; Zeng, P.; Pan, J. In vitro and in vivo studies on mucoadhesive microspheres of amoxicillin. *J. Control. Release* **2005**, *102*, 135–144. [CrossRef]
17. Franco, P.; Reverchon, E.; De Marco, I. Production of zein/antibiotic microparticles by supercritical antisolvent coprecipitation. *J. Supercrit. Fluids* **2019**, *145*, 31–38. [CrossRef]
18. Altman, R.; Bosch, B.; Brune, K.; Patrignani, P.; Young, C. Advances in NSAID development: Evolution of diclofenac products using pharmaceutical technology. *Drugs* **2015**, *75*, 859–877. [CrossRef]
19. Gupta, A.; Bah, M. NSAIDs in the treatment of postoperative pain. *Curr. Pain Headache Rep.* **2016**, *20*, 62. [CrossRef]
20. Maniar, K.H.; Jones, I.A.; Gopalakrishna, R.; Vangsness, C.T., Jr. Lowering side effects of NSAID usage in osteoarthritis: Recent attempts at minimizing dosage. *Expert Opin. Pharmacother.* **2018**, *19*, 93–102. [CrossRef]
21. Da Fonseca Machado, A.P.; Rezende, C.A.; Rodrigues, R.A.; Barbero, G.F.; e Rosa, P.d.T.V.; Martínez, J. Encapsulation of anthocyanin-rich extract from blackberry residues by spray-drying, freeze-drying and supercritical antisolvent. *Powder Technol.* **2018**, *340*, 553–562. [CrossRef]
22. Lee, C.-W.; Kim, S.-J.; Youn, Y.-S.; Widjojokusumo, E.; Lee, Y.-H.; Kim, J.; Lee, Y.-W.; Tjandrawinata, R.R. Preparation of bitter taste masked cetirizine dihydrochloride/β-cyclodextrin inclusion complex by supercritical antisolvent (SAS) process. *J. Supercrit. Fluids* **2010**, *55*, 348–357. [CrossRef]
23. Won, D.-H.; Kim, M.-S.; Lee, S.; Park, J.-S.; Hwang, S.-J. Improved physicochemical characteristics of felodipine solid dispersion particles by supercritical anti-solvent precipitation process. *Int. J. Pharm.* **2005**, *301*, 199–208. [CrossRef] [PubMed]
24. Park, H.; Seo, H.J.; Hong, S.-h.; Ha, E.-S.; Lee, S.; Kim, J.-S.; Baek, I.-h.; Kim, M.-S.; Hwang, S.-J. Characterization and therapeutic efficacy evaluation of glimepiride and L-arginine co-amorphous formulation prepared by supercritical antisolvent process: Influence of molar ratio and preparation methods. *Int. J. Pharm.* **2020**, *581*, 119232. [CrossRef] [PubMed]
25. Park, J.; Park, H.J.; Cho, W.; Cha, K.-H.; Kang, Y.-S.; Hwang, S.-J. Preparation and pharmaceutical characterization of amorphous cefdinir using spray-drying and SAS-process. *Int. J. Pharm.* **2010**, *396*, 239–245. [CrossRef] [PubMed]
26. Yeo, S.D.; Debenedetti, P.G.; Radosz, M.; Schmidt, H.W. Supercritical Antisolvent Process for Substituted Para-Linked Aromatic Polyamides: Phase Equilibrium and Morphology Study. *Macromolecules* **1993**, *26*, 6207–6210. [CrossRef]
27. Yeo, S.D.; Debenedetti, P.G.; Radosz, M.; Giesa, R.; Schmidt, H.W. Supercritical Antisolvent Process for a Series of Substituted Para-Linked Aromatic Polyamides. *Macromolecules* **1995**, *28*, 1316–1317. [CrossRef]
28. Bertucco, A.; Pallado, P.; Benedetti, L. Formation of biocompatible polymer microspheres for controlled drug delivery by a supercritical antisolvent technique. *Process Technol. Proc.* **1996**, *12*, 217–222.
29. Reverchon, E.; Della Porta, G.; Di Trolio, A.; Pace, S. Supercritical Antisolvent Precipitation of Nanoparticles of Superconductor Precursors. *Ind. Eng. Chem. Res.* **1998**, *37*, 952–958. [CrossRef]
30. Reverchon, E.; Celano, C.; Della Porta, G.; Di Trolio, A.; Pace, S. Supercritical antisolvent precipitation: A new technique for preparing submicronic yttrium powders to improve YBCO superconductor. *J. Mater. Res.* **1998**, *13*, 284–289. [CrossRef]

31. Chen, L.-F.; Xu, P.-Y.; Fu, C.-P.; Kankala, R.K.; Chen, A.-Z.; Wang, S.-B. Fabrication of Supercritical Antisolvent (SAS) Process-Assisted Fisetin-Encapsulated Poly (Vinyl Pyrrolidone)(PVP) Nanocomposites for Improved Anticancer Therapy. *Nanomaterials* **2020**, *10*, 322. [CrossRef] [PubMed]
32. Martin, T.M.; Bandi, N.; Shulz, R.; Roberts, C.B.; Kompella, U.B. Preparation of budesonide and budesonide-PLA microparticles using supercritical fluid precipitation technology. *AAPS PharmSciTech* **2002**, *3*, 16–26. [CrossRef] [PubMed]
33. Park, H.J.; Yoon, T.J.; Kwon, D.E.; Yu, K.; Lee, Y.-W. Coprecipitation of hydrochlorothiazide/PVP for the dissolution rate improvement by precipitation with compressed fluid antisolvent process. *J. Supercrit. Fluids* **2017**, *126*, 37–46. [CrossRef]
34. Ha, E.-S.; Choo, G.-H.; Baek, I.-h.; Kim, J.-S.; Cho, W.; Jung, Y.S.; Jin, S.-E.; Hwang, S.-J.; Kim, M.-S. Dissolution and bioavailability of lercanidipine–hydroxypropylmethyl cellulose nanoparticles with surfactant. *Int. J. Biol. Macromol.* **2015**, *72*, 218–222. [CrossRef]
35. Majerik, V.; Charbit, G.; Badens, E.; Horváth, G.; Szokonya, L.; Bosc, N.; Teillaud, E. Bioavailability enhancement of an active substance by supercritical antisolvent precipitation. *J. Supercrit. Fluids* **2007**, *40*, 101–110. [CrossRef]
36. Wang, Y.; Wang, Y.; Yang, J.; Pfeffer, R.; Dave, R.; Michniak, B. The application of a supercritical antisolvent process for sustained drug delivery. *Powder Technol.* **2006**, *164*, 94–102. [CrossRef]
37. Lee, S.; Kim, M.; Kim, J.; Park, H.; Woo, J.; Lee, B.; Hwang, S.J. Controlled delivery of a hydrophilic drug from a biodegradable microsphere system by supercritical anti-solvent precipitation technique. *J. Microencapsul.* **2006**, *23*, 741–749. [CrossRef]
38. Liu, M.; Liu, Y.; Ge, Y.; Zhong, Z.; Wang, Z.; Wu, T.; Zhao, X.; Zu, Y. Solubility, Antioxidation, and Oral Bioavailability Improvement of Mangiferin Microparticles Prepared Using the Supercritical Antisolvent Method. *Pharmaceutics* **2020**, *12*, 90. [CrossRef]
39. Ha, E.S.; Kim, J.S.; Baek, I.H.; Yoo, J.W.; Jung, Y.; Moon, H.R.; Kim, M.S. Development of megestrol acetate solid dispersion nanoparticles for enhanced oral delivery by using a supercritical antisolvent process. *Drug Des. Dev. Ther.* **2015**, *9*, 4269–4277.
40. Sacchetin, P.S.C.; Setti, R.F.; e Rosa, P.D.T.V.; Moraes, Â.M. Properties of PLA/PCL particles as vehicles for oral delivery of the androgen hormone 17α-methyltestosterone. *Mater. Sci. Eng. C* **2016**, *58*, 870–881. [CrossRef]
41. Jung, I.-I.; Haam, S.; Lim, G.; Ryu, J.-H. Preparation of peptide-loaded polymer microparticles using supercritical carbon dioxide. *Biotechnol. Bioprocess Eng.* **2012**, *17*, 185–194. [CrossRef]
42. Lee, S.; Nam, K.; Kim, M.S.; Jun, S.W.; Park, J.-S.; Woo, J.S.; Hwang, S.-J. Preparation and characterization of solid dispersions of itraconazole by using aerosol solvent extraction system for improvement in drug solubility and bioavailability. *Arch. Pharm. Res.* **2005**, *28*, 866–874. [CrossRef] [PubMed]
43. Duarte, A.R.C.; Roy, C.; Vega-González, A.; Duarte, C.M.; Subra-Paternault, P. Preparation of acetazolamide composite microparticles by supercritical anti-solvent techniques. *Int. J. Pharm.* **2007**, *332*, 132–139. [CrossRef] [PubMed]
44. Franco, P.; de Marco, I. Eudragit: A Novel Carrier for Controlled Drug Delivery in Supercritical Antisolvent Coprecipitation. *Polymers* **2020**, *12*, 234. [CrossRef] [PubMed]
45. Miguel, F.; Martín, A.; Mattea, F.; Cocero, M.J. Precipitation of lutein and co-precipitation of lutein and poly-lactic acid with the supercritical anti-solvent process. *Chem. Eng. Process.* **2008**, *47*, 1594–1602. [CrossRef]
46. Franco, P.; Reverchon, E.; De Marco, I. Zein/diclofenac sodium coprecipitation at micrometric and nanometric range by supercritical antisolvent processing. *J. CO2 Util.* **2018**, *27*, 366–373. [CrossRef]
47. Liu, G.; Li, S.; Huang, Y.; Wang, H.; Jiang, Y. Incorporation of 10-hydroxycamptothecin nanocrystals into zein microspheres. *Chem. Eng. Sci.* **2016**, *155*, 405–414. [CrossRef]
48. Zhong, Q.; Jin, M.; Davidson, P.M.; Zivanovic, S. Sustained release of lysozyme from zein microcapsules produced by a supercritical anti-solvent process. *Food Chem.* **2009**, *115*, 697–700. [CrossRef]
49. Hu, D.; Lin, C.; Liu, L.; Li, S.; Zhao, Y. Preparation, characterization, and in vitro release investigation of lutein/zein nanoparticles via solution enhanced dispersion by supercritical fluids. *J. Food Eng.* **2012**, *109*, 545–552. [CrossRef]
50. Abuzar, S.M.; Hyun, S.-M.; Kim, J.-H.; Park, H.J.; Kim, M.-S.; Park, J.-S.; Hwang, S.-J. Enhancing the solubility and bioavailability of poorly water-soluble drugs using supercritical antisolvent (SAS) process. *Int. J. Pharm.* **2018**, *538*, 1–13. [CrossRef]

51. Kalani, M.; Yunus, R. Application of supercritical antisolvent method in drug encapsulation: A review. *Int. J. Nanomed.* **2011**, *6*, 1429. [CrossRef] [PubMed]
52. Gonzalez-Coloma, A.; Martín, L.; Mainar, A.; Urieta, J.; Fraga, B.M.; Rodríguez-Vallejo, V.; Díaz, C.E. Supercritical extraction and supercritical antisolvent fractionation of natural products from plant material: Comparative results on Persea indica. *Phytochem. Rev.* **2012**, *11*, 433–446. [CrossRef]
53. Reverchon, E. Supercritical antisolvent precipitation of micro-and nano-particles. *J. Supercrit. Fluids* **1999**, *15*, 1–21. [CrossRef]
54. Savjani, K.T.; Gajjar, A.K.; Savjani, J.K. Drug solubility: Importance and enhancement techniques. *ISRN Pharm.* **2012**, *2012*, 195727. [CrossRef] [PubMed]
55. Vieth, M.; Siegel, M.G.; Higgs, R.E.; Watson, I.A.; Robertson, D.H.; Savin, K.A.; Durst, G.L.; Hipskind, P.A. Characteristic physical properties and structural fragments of marketed oral drugs. *J. Med. Chem.* **2004**, *47*, 224–232. [CrossRef]
56. Rodriguez-Aller, M.; Guillarme, D.; Veuthey, J.-L.; Gurny, R. Strategies for formulating and delivering poorly water-soluble drugs. *J. Drug Deliv. Sci. Technol.* **2015**, *30*, 342–351. [CrossRef]
57. Takagi, T.; Ramachandran, C.; Bermejo, M.; Yamashita, S.; Yu, L.X.; Amidon, G.L. A provisional biopharmaceutical classification of the top 200 oral drug products in the United States, Great Britain, Spain, and Japan. *J. CO2 Util. Pharm.* **2006**, *3*, 631–643. [CrossRef]
58. Tenorio, A.; Gordillo, M.D.; Pereyra, C.; Martinez de la Ossa, E.J. Controlled submicro particle formation of ampicillin by supercritical antisolvent precipitation. *J. Supercrit. Fluids* **2007**, *40*, 308–316. [CrossRef]
59. Kalogiannis, C.G.; Pavlidou, E.; Panayiotou, C.G. Production of amoxicillin microparticles by supercritical antisolvent precipitation. *Ind. Eng. Chem. Res.* **2005**, *44*, 9339–9346. [CrossRef]
60. Reverchon, E.; Della Porta, G.; Falivene, M. Process parameters and morphology in amoxicillin micro and submicro particles generation by supercritical antisolvent precipitation. *J. Supercrit. Fluids* **2000**, *17*, 239–248. [CrossRef]
61. Reverchon, E.; De Marco, I. Supercritical antisolvent precipitation of cephalosporins. *Powder Technol.* **2006**, *164*, 139–146. [CrossRef]
62. Reverchon, E.; De Marco, I.; Della Porta, G. Rifampicin microparticles production by supercritical antisolvent precipitation. *Int. J. Pharm.* **2002**, *243*, 83–91. [CrossRef]
63. Cardoso, M.T.; Monteiro, G.; Cardoso, J.; Prazeres, T.; Figueiredo, J.; Martinho, J.; Cabral, J.; Palavra, A. Supercritical antisolvent micronization of minocycline hydrochloride. *J. Supercrit. Fluids* **2008**, *44*, 238–244. [CrossRef]
64. Cardoso, M.T.; Geraldes, V.; Cabral, J.; Palavra, A. Characterization of minocycline powder micronized by a supercritical antisolvent (SAS) process. *J. Supercrit. Fluids* **2008**, *46*, 71–76. [CrossRef]
65. Franco, P.; Reverchon, E.; De Marco, I. PVP/ketoprofen coprecipitation using supercritical antisolvent process. *Powder Technol.* **2018**, *340*, 1–7. [CrossRef]
66. Montes, A.; Wehner, L.; Pereyra, C.; Martínez de la Ossa, E.J. Mangiferin nanoparticles precipitation by supercritical antisolvent process. *J. Supercrit. Fluids* **2016**, *112*, 44–50. [CrossRef]
67. Cuadra, I.A.; Zahran, F.; Martín, D.; Cabañas, A.; Pando, C. Preparation of 5-fluorouracil microparticles and 5-fluorouracil/poly(l-lactide) composites by a supercritical CO_2 antisolvent process. *J. Supercrit. Fluids* **2019**, *143*, 64–71. [CrossRef]
68. Widjojokusumo, E.; Veriansyah, B.; Tjandrawinata, R.R. Supercritical anti-solvent (SAS) micronization of Manilkara kauki bioactive fraction (DLBS2347). *J. CO2 Util.* **2013**, *3-4*, 30–36. [CrossRef]
69. Zhao, X.; Chen, X.; Zu, Y.; Jiang, R.; Zhao, D. Recrystallization and micronization of taxol using the supercritical antisolvent (SAS) process. *Ind. Eng. Chem. Res.* **2012**, *51*, 9591–9597. [CrossRef]
70. Park, J.; Cho, W.; Cha, K.-H.; Ahn, J.; Han, K.; Hwang, S.-J. Solubilization of the poorly water soluble drug, telmisartan, using supercritical anti-solvent (SAS) process. *Int. J. Pharm.* **2013**, *441*, 50–55. [CrossRef]
71. Reverchon, E.; Della Porta, G.; Pallado, P. Supercritical antisolvent precipitation of salbutamol microparticles. *Powder Technol.* **2001**, *114*, 17–22. [CrossRef]
72. Kim, M.-S.; Jin, S.-J.; Kim, J.-S.; Park, H.J.; Song, H.-S.; Neubert, R.H.; Hwang, S.-J. Preparation, characterization and in vivo evaluation of amorphous atorvastatin calcium nanoparticles using supercritical antisolvent (SAS) process. *Eur. J. Pharm. Biopharm.* **2008**, *69*, 454–465. [CrossRef] [PubMed]

73. Rogers, T.L.; Johnston, K.P.; Williams, R.O., III. Solution-based particle formation of pharmaceutical powders by supercritical or compressed fluid CO_2 and cryogenic spray-freezing technologies. *Drug Dev. Ind. Pharm.* **2001**, *27*, 1003–1015. [CrossRef] [PubMed]
74. Chang, Y.-P.; Tang, M.; Chen, Y.-P. Micronization of sulfamethoxazole using the supercritical anti-solvent process. *J. Mater. Sci.* **2008**, *43*, 2328–2335. [CrossRef]
75. Hiendrawan, S.; Veriansyah, B.; Widjojokusumo, E.; Soewandhi, S.; Wikarsa, S.; Tjandrawinata, R.R. Simultaneous cocrystallization and micronization of paracetamol-dipicolinic acid cocrystal by supercritical antisolvent (SAS). *Int. J. Pharm. Pharm. Sci.* **2016**, *8*, 89–98.
76. Kim, M.-S.; Lee, S.; Park, J.-S.; Woo, J.-S.; Hwang, S.-J. Micronization of cilostazol using supercritical antisolvent (SAS) process: Effect of process parameters. *Powder Technol.* **2007**, *177*, 64–70. [CrossRef]
77. Kudryashova, E.; Sukhoverkov, K.; Deygen, I.; Vorobei, A.; Pokrovskiy, O.; Parenago, O.; Presnov, D.; Egorov, A. Moxifloxacin Micronization via Supercritical Antisolvent Precipitation. *Russ. J. Phys. Chem. B* **2017**, *11*, 1153–1162. [CrossRef]
78. Visentin, A.; Rodríguez-Rojo, S.; Navarrete, A.; Maestri, D.; Cocero, M.J. Precipitation and encapsulation of rosemary antioxidants by supercritical antisolvent process. *J. Food Eng.* **2012**, *109*, 9–15. [CrossRef]
79. De Marco, I.; Prosapio, V.; Cice, F.; Reverchon, E. Use of solvent mixtures in supercritical antisolvent process to modify precipitates morphology: Cellulose acetate microparticles. *J. Supercrit. Fluids* **2013**, *83*, 153–160. [CrossRef]
80. Matos, R.L.; Lu, T.; Prosapio, V.; McConville, C.; Leeke, G.; Ingram, A. Coprecipitation of curcumin/PVP with enhanced dissolution properties by the supercritical antisolvent process. *J. CO2 Util.* **2019**, *30*, 48–62. [CrossRef]
81. Prosapio, V.; Reverchon, E.; De Marco, I. Coprecipitation of polyvinylpyrrolidone/β-carotene by supercritical antisolvent processing. *Ind. Eng. Chem. Res.* **2015**, *54*, 11568–11575. [CrossRef]
82. Campardelli, R.; Reverchon, E.; De Marco, I. Dependence of SAS particle morphologies on the ternary phase equilibria. *J. Supercrit. Fluids* **2017**, *130*, 273–281. [CrossRef]
83. Campardelli, R.; Reverchon, E.; De Marco, I. PVP microparticles precipitation from acetone-ethanol mixtures using SAS process: Effect of phase behavior. *J. Supercrit. Fluids* **2019**, *143*, 321–329. [CrossRef]
84. Martín, A.n.; Scholle, K.; Mattea, F.; Meterc, D.; Cocero, M.a.J. Production of polymorphs of ibuprofen sodium by supercritical antisolvent (SAS) precipitation. *Cryst. Growth Des.* **2009**, *9*, 2504–2511. [CrossRef]
85. Reverchon, E.; Della Porta, G. Production of antibiotic micro-and nano-particles by supercritical antisolvent precipitation. *Powder Technol.* **1999**, *106*, 23–29. [CrossRef]
86. Chattopadhyay, P.; Gupta, R.B. Production of griseofulvin nanoparticles using supercritical CO2 antisolvent with enhanced mass transfer. *Int. J. Pharm.* **2001**, *228*, 19–31. [CrossRef]
87. Bagratashvili, V.; Egorov, A.; Krotova, L.; Mironov, A.; Panchenko, V.Y.; Parenago, O.; Popov, V.; Revelsky, I.; Timashev, P.; Tsypina, S. Supercritical fluid micronization of risperidone pharmaceutical substance. *Russ. J. Phys. Chem. B* **2012**, *6*, 804–812. [CrossRef]
88. Su, C.S.; Lo, W.S.; Lien, L.H. Micronization of fluticasone propionate using supercritical antisolvent (SAS) process. *Chem. Eng. Technol.* **2011**, *34*, 535–541. [CrossRef]
89. Quintana, S.E.; Hernández, D.M.; Villanueva-Bermejo, D.; García-Risco, M.R.; Fornari, T. Fractionation and precipitation of licorice (Glycyrrhiza glabra L.) phytochemicals by supercritical antisolvent (SAS) technique. *LWT* **2020**, 109315. [CrossRef]
90. Miguel, F.; Martin, A.; Gamse, T.; Cocero, M.J. Supercritical anti solvent precipitation of lycopene: Effect of the operating parameters. *J. Supercrit. Fluids* **2006**, *36*, 225–235. [CrossRef]
91. Fernández-Ponce, M.T.; Masmoudi, Y.; Djerafi, R.; Casas, L.; Mantell, C.; de La Ossa, E.M.; Badens, E. Particle design applied to quercetin using supercritical anti-solvent techniques. *J. Supercrit. Fluids* **2015**, *105*, 119–127. [CrossRef]
92. Montes, A.; Pereyra, C.; de la Ossa, E.M. Screening design of experiment applied to the supercritical antisolvent precipitation of quercetin. *J. Supercrit. Fluids* **2015**, *104*, 10–18. [CrossRef]
93. Prosapio, V.; De Marco, I.; Reverchon, E. PVP/corticosteroid microspheres produced by supercritical antisolvent coprecipitation. *Chem. Eng. J.* **2016**, *292*, 264–275. [CrossRef]
94. Prosapio, V.; De Marco, I.; Scognamiglio, M.; Reverchon, E. Folic acid–PVP nanostructured composite microparticles by supercritical antisolvent precipitation. *Chem. Eng. J.* **2015**, *277*, 286–294. [CrossRef]

95. Franceschi, E.; De Cesaro, A.M.; Feiten, M.; Ferreira, S.R.S.; Dariva, C.; Kunita, M.H.; Rubira, A.F.; Muniz, E.C.; Corazza, M.L.; Oliveira, J.V. Precipitation of β-carotene and PHBV and co-precipitation from SEDS technique using supercritical CO_2. *J. Supercrit. Fluids* **2008**, *47*, 259–269. [CrossRef]
96. Priamo, W.L.; De Cezaro, A.M.; Ferreira, S.R.S.; Oliveira, J.V. Precipitation and encapsulation of β-carotene in PHBV using carbon dioxide as anti-solvent. *J. Supercrit. Fluids* **2010**, *54*, 103–109. [CrossRef]
97. Ozkan, G.; Franco, P.; Capanoglu, E.; De Marco, I. PVP/flavonoid coprecipitation by supercritical antisolvent process. *Chem. Eng. Process.* **2019**, *146*, 107689. [CrossRef]
98. Montes, A.; Kin, N.; Gordillo, M.D.; Pereyra, C.; Martínez de la Ossa, E.J. Polymer–naproxen precipitation by supercritical antisolvent (SAS) process. *J. Supercrit. Fluids* **2014**, *89*, 58–67. [CrossRef]
99. Montes, A.; Gordillo, M.D.; Pereyra, C.; De los Santos, D.M.; Martínez de la Ossa, E.J. Ibuprofen–polymer precipitation using supercritical CO_2 at low temperature. *J. Supercrit. Fluids* **2014**, *94*, 91–101. [CrossRef]
100. Montes, A.; Gordillo, M.D.; Pereyra, C.; Martínez de la Ossa, E.J. Polymer and ampicillin co-precipitation by supercritical antisolvent process. *J. Supercrit. Fluids* **2012**, *63*, 92–98. [CrossRef]
101. Montes, A.; Nunes, A.; Gordillo, M.; Pereyra, C.; Duarte, C.M.; Martinez de la Ossa, E.J. Amoxicillin and ethyl cellulose precipitation by two supercritical antisolvent processes. *Chem. Eng. Technol.* **2013**, *36*, 665–672. [CrossRef]
102. Montes, A.; Gordillo, M.D.; Pereyra, C.; Martínez de la Ossa, E.J. Co-precipitation of amoxicillin and ethyl cellulose microparticles by supercritical antisolvent process. *J. Supercrit. Fluids* **2011**, *60*, 75–80. [CrossRef]
103. Uzun, İ.N.; Sipahigil, O.; Dinçer, S. Coprecipitation of Cefuroxime Axetil–PVP composite microparticles by batch supercritical antisolvent process. *J. Supercrit. Fluids* **2011**, *55*, 1059–1069. [CrossRef]
104. De Marco, I.; Franco, P. Production of Eudragit/ampicillin Microparticles by Supercritical Antisolvent Coprecipitation. *Chem. Eng. Trans.* **2020**, *79*, 229–234.
105. Djerafi, R.; Swanepoel, A.; Crampon, C.; Kalombo, L.; Labuschagne, P.; Badens, E.; Masmoudi, Y. Supercritical antisolvent co-precipitation of rifampicin and ethyl cellulose. *Eur. J. Pharm. Sci.* **2017**, *102*, 161–171. [CrossRef]
106. Barrett, A.M.; Dehghani, F.; Foster, N.R. Increasing the Dissolution Rate of Itraconazole Processed by Gas Antisolvent Techniques using Polyethylene Glycol as a Carrier. *Pharm. Res.* **2007**, *25*, 1274–1289. [CrossRef]
107. Jin, H.Y.; Xia, F.; Zhao, Y.P. Preparation of hydroxypropyl methyl cellulose phthalate nanoparticles with mixed solvent using supercritical antisolvent process and its application in co-precipitation of insulin. *Adv. Powder Technol.* **2012**, *23*, 157–163. [CrossRef]
108. Elvassore, N.; Bertucco, A.; Caliceti, P. Production of protein-loaded polymeric microcapsules by compressed CO_2 in a mixed solvent. *Ind. Eng. Chem. Res.* **2001**, *40*, 795–800. [CrossRef]
109. Kalantarian, P.; Haririan, I.; Najafabadi, A.R.; Shokrgozar, M.A.; Vatanara, A. Entrapment of 5-fluorouracil into PLGA matrices using supercritical antisolvent processes. *J. Pharm. Pharmacol.* **2011**, *63*, 500–506. [CrossRef]
110. Ha, E.-S.; Kim, J.-S.; Baek, I.-h.; Hwang, S.-J.; Kim, M.-S. Enhancement of dissolution and bioavailability of ezetimibe by amorphous solid dispersion nanoparticles fabricated using supercritical antisolvent process. *J. Pharm. Investig.* **2015**, *45*, 641–649. [CrossRef]
111. Argemí, A.; Vega, A.; Subra-Paternault, P.; Saurina, J. Characterization of azacytidine/poly(l-lactic) acid particles prepared by supercritical antisolvent precipitation. *J. Pharm. Biomed. Anal.* **2009**, *50*, 847–852. [CrossRef] [PubMed]
112. Chen, A.Z.; Pu, X.M.; Kang, Y.Q.; Liao, L.; Yao, Y.D.; Yin, G.F. Preparation of 5–Fluorouracil–Poly (L–lactide) Microparticles Using Solution–Enhanced Dispersion by Supercritical CO_2. *Macromol. Rapid Commun.* **2006**, *27*, 1254–1259. [CrossRef]
113. Alias, D.; Yunus, R.; Chong, G.H.; Che Abdullah, C.A. Single step encapsulation process of tamoxifen in biodegradable polymer using supercritical anti-solvent (SAS) process. *Powder Technol.* **2017**, *309*, 89–94. [CrossRef]
114. Huang, Y.; Zu, Y.; Zhao, X.; Wu, M.; Feng, Z.; Deng, Y.; Zu, C.; Wang, L. Preparation of inclusion complex of apigenin-hydroxypropyl-β-cyclodextrin by using supercritical antisolvent process for dissolution and bioavailability enhancement. *Int. J. Pharm.* **2016**, *511*, 921–930. [CrossRef]
115. Lestari, S.D.; Machmudah, S.; Winardi, S.; Kanda, H.; Goto, M. Particle micronization of Curcuma mangga rhizomes ethanolic extract/biopolymer PVP using supercritical antisolvent process. *J. Supercrit. Fluids* **2019**, *146*, 226–239. [CrossRef]

116. Pan, Y.-J.; Xu, P.-Y.; Chen, B.-Q.; Fu, C.-P.; Kankala, R.K.; Chen, A.-Z.; Wang, S.-B. Supercritical Antisolvent Process-assisted Fabrication of Chrysin-polyvinylpyrrolidone Sub-microparticles for Improved Anticancer Efficiency. *J. Supercrit. Fluids* **2020**, *162*, 104847. [CrossRef]
117. Machmudah, S.; Winardi, S.; Wahyudiono; Kanda, H.; Goto, M. Formation of Fine Particles from Curcumin/PVP by the Supercritical Antisolvent Process with a Coaxial Nozzle. *ACS Omega* **2020**, *5*, 6705–6714. [CrossRef]
118. Wang, W.; Liu, G.; Wu, J.; Jiang, Y. Co-precipitation of 10-hydroxycamptothecin and poly (L-lactic acid) by supercritical CO_2 anti-solvent process using dichloromethane/ethanol co-solvent. *J. Supercrit. Fluids* **2013**, *74*, 137–144. [CrossRef]
119. Patomchaiviwat, V.; Paeratakul, O.; Kulvanich, P. Formation of inhalable rifampicin–poly (L-lactide) microparticles by supercritical anti-solvent process. *AAPS PharmSciTech* **2008**, *9*, 1119–1129. [CrossRef]
120. Yoshida, V.M.H.; Balcão, V.M.; Vila, M.M.D.C.; Oliveira Júnior, J.M.; Aranha, N.; Chaud, M.V.; Gremião, M.P.D. Zidovudine-Poly(L-Lactic Acid) Solid Dispersions with Improved Intestinal Permeability Prepared by Supercritical Antisolvent Process. *J. Pharm. Sci.* **2015**, *104*, 1691–1700. [CrossRef]
121. Lin, Q.; Liu, G.; Zhao, Z.; Wei, D.; Pang, J.; Jiang, Y. Design of gefitinib-loaded poly (L-lactic acid) microspheres via a supercritical anti-solvent process for dry powder inhalation. *Int. J. Pharm.* **2017**, *532*, 573–580. [CrossRef] [PubMed]
122. Montes, A.; Wehner, L.; Pereyra, C.; Martínez de la Ossa, E.J. Generation of microparticles of ellagic acid by supercritical antisolvent process. *J. Supercrit. Fluids* **2016**, *116*, 101–110. [CrossRef]
123. Chhouk, K.; Kanda, H.; Kawasaki, S.-I.; Goto, M. Micronization of curcumin with biodegradable polymer by supercritical anti-solvent using micro swirl mixer. *Front. Chem. Sci. Eng.* **2018**, *12*, 184–193. [CrossRef]
124. Guha, R.; Vinjamur, M.; Mukhopadhyay, M. Demonstration of mechanisms for coprecipitation and encapsulation by supercritical antisolvent process. *Ind. Eng. Chem. Res.* **2011**, *50*, 1079–1088. [CrossRef]
125. Kalogiannis, C.G.; Michailof, C.M.; Panayiotou, C.G. Microencapsulation of amoxicillin in poly (l-lactic acid) by supercritical antisolvent precipitation. *Ind. Eng. Chem. Res.* **2006**, *45*, 8738–8743. [CrossRef]
126. Li, W.; Liu, G.; Li, L.; Wu, J.; LÜ, Y.; Jiang, Y. Effect of Process Parameters on Co-precipitation of Paclitaxel and Poly(L-lactic Acid) by Supercritical Antisolvent Process. *Chin. J. Chem. Eng.* **2012**, *20*, 803–813. [CrossRef]
127. Liu, G.; Hu, M.; Zhao, Z.; Lin, Q.; Wei, D.; Jiang, Y. Enhancing the stability of astaxanthin by encapsulation in poly (L-lactic acid) microspheres using a supercritical anti-solvent process. *Particuology* **2019**, *44*, 54–62. [CrossRef]
128. Nerome, H.; Machmudah, S.; Wahyudiono; Fukuzato, R.; Higashiura, T.; Youn, Y.S.; Lee, Y.W.; Goto, M. Nanoparticle formation of lycopene/β-cyclodextrin inclusion complex using supercritical antisolvent precipitation. *J. Supercrit. Fluids* **2013**, *83*, 97–103. [CrossRef]
129. Martín, A.; Mattea, F.; Gutiérrez, L.; Miguel, F.; Cocero, M.J. Co-precipitation of carotenoids and bio-polymers with the supercritical anti-solvent process. *J. Supercrit. Fluids* **2007**, *41*, 138–147. [CrossRef]
130. Lang, Z.M.; Hong, H.L.; Han, L.M.; Zhu, N.; Suo, Q.L. Preparation of emodin-polyethylene glycol composite microparticles using a supercritical antisolvent process. *Chem. Eng. Technol.* **2012**, *35*, 362–368. [CrossRef]
131. Machado, F.R.S.; Trevisol, T.C.; Boschetto, D.L.; Burkert, J.F.M.; Ferreira, S.R.S.; Oliveira, J.V.; Burkert, C.A.V. Technological process for cell disruption, extraction and encapsulation of astaxanthin from Haematococcus pluvialis. *J. Biotechnol.* **2016**, *218*, 108–114. [CrossRef] [PubMed]
132. Boschetto, D.L.; Aranha, E.M.; de Souza, A.A.U.; Souza, S.M.A.G.U.; Ferreira, S.R.S.; Priamo, W.L.; Oliveira, J.V. Encapsulation of bixin in PHBV using SEDS technique and in vitro release evaluation. *Ind Crops Prod.* **2014**, *60*, 22–29. [CrossRef]
133. Boschetto, D.L.; Dalmolin, I.; de Cesaro, A.M.; Rigo, A.A.; Ferreira, S.R.S.; Meireles, M.A.A.; Batista, E.A.C.; Vladimir Oliveira, J. Phase behavior and process parameters effect on grape seed extract encapsulation by SEDS technique. *Ind. Crops Prod.* **2013**, *50*, 352–360. [CrossRef]
134. Andrade, K.S.; Aguiar, G.P.S.; Rebelatto, E.A.; Lanza, M.; Oliveira, J.V.; Ferreira, S.R. Encapsulation of pink pepper extract by SEDS technique: Phase behavior data and process parameters. *J. Supercrit. Fluids* **2020**, *161*, 104822. [CrossRef]
135. Franceschi, E.; De Cezaro, A.; Ferreira, S.R.S.; Kunita, M.H.; Muniz, E.C.; Rubira, A.F.; Oliveira, J.V. Co-precipitation of beta-carotene and bio-polymer using supercritical carbon dioxide as antisolvent. *Open Chem. Eng. J.* **2010**, *4*, 11–20. [CrossRef]

136. Lee, S.Y.; Abdullah, L.C.; Rahman, R.A.; Abas, F.; Chong, G.H. Role of polymers as crystal growth inhibitors in coprecipitation via solution-enhanced dispersion by supercritical fluids (SEDS) to improve andrographolide dissolution from standardized Andrographis paniculata extract. *J. Drug Deliv. Sci. Technol.* **2019**, *50*, 145–154. [CrossRef]
137. Zhou, R.; Wang, F.; Guo, Z.; Zhao, Y. Preparation and characterization of resveratrol/hydroxypropyl–β–cyclodextrin inclusion complex using supercritical antisolvent technology. *J. Food Process Eng.* **2012**, *35*, 677–686. [CrossRef]
138. Yan, T.; Ji, M.; Sun, Y.; Yan, T.; Zhao, J.; Zhang, H.; Wang, Z. Preparation and characterization of baicalein/hydroxypropyl-β-cyclodextrin inclusion complex for enhancement of solubility, antioxidant activity and antibacterial activity using supercritical antisolvent technology. *J. Incl. Phenom. Macrocycl. Chem.* **2020**, *96*, 285–295. [CrossRef]
139. Sun, J.; Hong, H.; Zhu, N.; Han, L.; Suo, Q. Response surface methodology to optimize the preparation of tosufloxacin tosylate/hydroxypropyl-β-cyclodextrin inclusion complex by supercritical antisolvent process. *J. Mol. Struct.* **2019**, *1198*, 126939. [CrossRef]
140. Jun, S.W.; Kim, M.-S.; Kim, J.-S.; Park, H.J.; Lee, S.; Woo, J.-S.; Hwang, S.-J. Preparation and characterization of simvastatin/hydroxypropyl-β-cyclodextrin inclusion complex using supercritical antisolvent (SAS) process. *Eur. J. Pharm. Biopharm.* **2007**, *66*, 413–421. [CrossRef]
141. Zhong, Q.; Jin, M. Nanoscalar structures of spray-dried zein microcapsules and in vitro release kinetics of the encapsulated lysozyme as affected by formulations. *J. Agric. Food Chem.* **2009**, *57*, 3886–3894. [CrossRef] [PubMed]
142. Quispe-Condori, S.; Saldaña, M.D.; Temelli, F. Microencapsulation of flax oil with zein using spray and freeze drying. *LWT-Food Sci. Technol.* **2011**, *44*, 1880–1887. [CrossRef]
143. Wang, L.; Zhang, Y. Eugenol nanoemulsion stabilized with zein and sodium caseinate by self-assembly. *J. Agric. Food Chem.* **2017**, *65*, 2990–2998. [CrossRef] [PubMed]
144. Tu, L.S.; Dehghani, F.; Foster, N. Micronisation and microencapsulation of pharmaceuticals using a carbon dioxide antisolvent. *Powder Technol.* **2002**, *126*, 134–149. [CrossRef]
145. Kikic, I.; Vecchione, F. Supercritical impregnation of polymers. *Curr. Opin. Solid State Mater. Sci.* **2003**, *7*, 399–405. [CrossRef]
146. Lian, Z.; Epstein, S.A.; Blenk, C.W.; Shine, A.D. Carbon dioxide-induced melting point depression of biodegradable semicrystalline polymers. *J. Supercrit. Fluids* **2006**, *39*, 107–117. [CrossRef]
147. Liu, G.; Wei, D.; Wang, H.; Hu, Y.; Jiang, Y. Self-assembly of zein microspheres with controllable particle size and narrow distribution using a novel built-in ultrasonic dialysis process. *Chem. Eng. J.* **2016**, *284*, 1094–1105. [CrossRef]
148. Rosa, M.T.M.; Alvarez, V.H.; Albarelli, J.Q.; Santos, D.T.; Meireles, M.A.A.; Saldaña, M.D. Supercritical Anti-solvent Process as an Alternative Technology for Vitamin Complex Encapsulation Using Zein as Wall Material: Technical-economic Evaluation. *J. Supercrit. Fluids* **2019**. [CrossRef]
149. He, W.; Suo, Q.; Hong, H.; Shan, A.; Li, C.; Huang, Y.; Li, Y.; Zhu, M. Production of natural carotene-dispersed polymer microparticles by SEDS-PA co-precipitation. *J. Mater. Sci.* **2007**, *42*, 3495–3501. [CrossRef]
150. Mezzomo, N.; Paz, E.d.; Maraschin, M.; Martín, Á.; Cocero, M.J.; Ferreira, S.R.S. Supercritical anti-solvent precipitation of carotenoid fraction from pink shrimp residue: Effect of operational conditions on encapsulation efficiency. *J. Supercrit. Fluids* **2012**, *66*, 342–349. [CrossRef]
151. Fraile, M.; Buratto, R.; Gómez, B.; Martín, Á.; Cocero, M.J. Enhanced Delivery of Quercetin by Encapsulation in Poloxamers by Supercritical Antisolvent Process. *Ind. Eng. Chem. Res.* **2014**, *53*, 4318–4327. [CrossRef]
152. García-Casas, I.; Montes, A.; Pereyra, C.; Martínez de la Ossa, E.J. Generation of quercetin/cellulose acetate phthalate systems for delivery by supercritical antisolvent process. *Eur. J. Pharm. Sci.* **2017**, *100*, 79–86. [CrossRef] [PubMed]
153. García-Casas, I.; Montes, A.; Pereyra, C.; Martínez De La Ossa, E.J. Co-precipitation of mangiferin with cellulose acetate phthalate by supercritical antisolvent process. *J. CO2 Util.* **2017**, *22*, 197–207. [CrossRef]
154. Ober, C.A.; Kalombo, L.; Swai, H.; Gupta, R.B. Preparation of rifampicin/lactose microparticle composites by a supercritical antisolvent-drug excipient mixing technique for inhalation delivery. *Powder Technol.* **2013**, *236*, 132–138. [CrossRef]

155. Cheng, Y.-S.; Lu, P.-M.; Huang, C.-Y.; Wu, J.-J. Encapsulation of lycopene with lecithin and α-tocopherol by supercritical antisolvent process for stability enhancement. *J. Supercrit. Fluids* **2017**, *130*, 246–252. [CrossRef]
156. Elizondo, E.; Sala, S.; Imbuluzqueta, E.; González, D.; Blanco-Prieto, M.J.; Gamazo, C.; Ventosa, N.; Veciana, J. High loading of gentamicin in bioadhesive PVM/MA nanostructured microparticles using compressed carbon-dioxide. *Pharm. Res.* **2011**, *28*, 309–321. [CrossRef]
157. Junior, O.V.; Cardoso, F.A.R.; Giufrida, W.M.; de Souza, M.F.; Cardozo-Filho, L. Production and computational fluid dynamics-based modeling of PMMA nanoparticles impregnated with ivermectin by a supercritical antisolvent process. *J. CO2 Util.* **2020**, *35*, 47–58. [CrossRef]
158. Cuadra, I.A.; Cabañas, A.; Cheda, J.A.; Türk, M.; Pando, C. Cocrystallization of the anticancer drug 5-fluorouracil and coformers urea, thiourea or pyrazinamide using supercritical CO2 as an antisolvent (SAS) and as a solvent (CSS). *J. Supercrit. Fluids* **2020**, 104813. [CrossRef]
159. Saad, S.; Ahmad, I.; Kawish, S.M.; Khan, U.A.; Ahmad, F.J.; Ali, A.; Jain, G.K. Improved cardioprotective effects of hesperidin solid lipid nanoparticles prepared by supercritical antisolvent technology. *Colloids Surf. B Biointerfaces* **2020**, *187*, 110628. [CrossRef]
160. Padrela, L.; Rodrigues, M.A.; Velaga, S.P.; Matos, H.A.; de Azevedo, E.G. Formation of indomethacin–saccharin cocrystals using supercritical fluid technology. *Eur. J. Pharm. Sci.* **2009**, *38*, 9–17. [CrossRef]

© 2020 by the authors. Licensee MDPI, Basel, Switzerland. This article is an open access article distributed under the terms and conditions of the Creative Commons Attribution (CC BY) license (http://creativecommons.org/licenses/by/4.0/).